Au NANO- AND MICROANTENNA ARRAYS FOR SENSOR APPLICATIONS FROM MID-INFRARED TO TERAHERTZ

A.G. Milekhin[a, b], E.E. Rodyakina[a,b], S.A. Kuznetsov[b], I.A. Milekhin[a,b], M.M. Kachanova[a], L.L. Sveshnikova[a], V.M. Dzhagan[c], A.V. Latyshev[a,b], and D.R.T. Zahn[c]

[a]*A.V. Rzhanov Institute of Semiconductor Physics, Lavrentjeva, 13, 630090, Novosibirsk, Russia*

[b]*Novosibirsk State University, Pirogov str. 2, 630090, Novosibirsk, Russia*
[c]*Semiconductor Physics, D-09107 Chemnitz, Technische Universität Chemnitz, Germany*

Energies of localised surface plasmon resonances (LSPR's) in metal nanostructures can be located in the spectral range from ultra-violet to terahertz depending on their size and morphology. It allows them as key element for surface-enhanced infrared absorption (SEIRA) by organic and inorganic materials to be used.

Here we present the results of an investigation of SEIRA by semiconductor nanocrystals (NCs) and organic substances homogeneously deposited on arrays of Au antennas and show the effectiveness of antenna for detection of an ultra-low amount of matter.

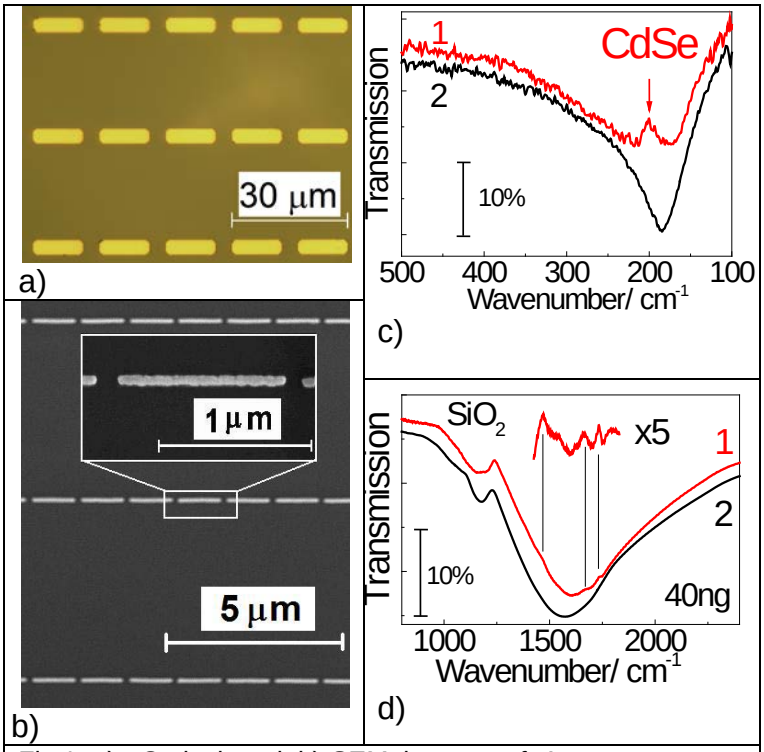

Fig.1 a)- Optical and b)-SEM images of Au nanoantenna arrays. SEIRA spectra of c)- 1 monolayer of CdSe nanocrystals and d)- 40 ng of cortisol. The IR spectra of the virgin arrays (curves 2) are given for comparison.

Nano- and optical lithography was employed to fabricate Au antenna arrays on a Si surface with specific structural parameters, i.e. length and width (Fig.1a,b), providing an energy of the localised surface plasmon resonance (LSPR) close to that of the most intensive vibrational modes in the organic molecules and optical phonons in semiconductor NCs (Fig.1c,d). The structural parameters of Au antennas were determined by scanning electron (SEM) and optical microscopy. The LSPR energy in the arrays of Au antennas as a function of their size was determined by means of IR spectroscopy. The potential of nanoantenna arrays for determining the cortisol concentration in real biological samples is discussed.

This work was supported by Russian Science Foundation (project 14-12-01037).

Keywords: enhancement; IR absorption; phonons

THE INFLUENCE OF DOPANT LOCALIZATION ON THE LUMINESCENCE PROPERTIES OF Ce(III) AND Eu(II)-DOPED ZnS AND SrS NANOPARTICLES.

Selyshchev Oleksandr, Pavlishchuk Vitaly

L. V. Pisarzhevskii Institute of Physical Chemistry of the National Academy of Sciences of Ukraine, Prospekt Nauky 31, Kyiv, 03028, Ukraine.

Luminescence of semiconductor and dielectric nanoparticles doped with rare earth ions are of interest due to their potential applications as biomedical sensors and as fluorescent components in color screens and white light emitting devices (LEDs) [1,2]. One of the fundamental problems associated with doped nanoparticles is the influence on their properties of the large percentage of surface atoms. In current study we try to answer what way the location of Ce(III) and Eu(II) in a volume or on a surface will influence on their luminescence by doping of zinc and strontium sulfides nanoparticles.

Nanoparticles were obtained by single source precursor method by decomposition of dithiocarbamate complexes of Strontium, Zinc, Europium (III) and Cerium (III) in high boiling point solvents. By successive addition of complexes in reaction mixture there were synthesized two series of nanoparticles: ZnS@Eu^{2+}, SrS@Eu^{2+}, SrS@Ce^{3+} and ZnS@Eu^{2+}@ZnS, SrS@Eu^{2+}@SrS, SrS@Ce^{3+}@SrS where the ions of dopants are localized respectively on the surface and in the volume between the core and the shell layers consisting of the same substances.

For ZnS@Eu^{2+} nanoparticles it was observed a red luminescence at 645 nm, whereas for ZnS@Eu^{2+}@ZnS luminescence was vanished. So one can conclude that luminescence of ZnS activated by Eu^{2+} is caused by surface location of Eu^{2+}.

In a case of SrS activated by Eu^{2+} a red luminescence was observed for both SrS@Eu^{2+}@SrS and SrS@Eu^{2+} nanoparticles with emission maxima at 610 and 580 nm respectively. In excitation spectra of SrS@Eu^{2+}@SrS it was found two bands attributed to own Eu^{2+} 4f–5d electronic transitions and probably to SrS host excitation with subsequent energy transfer on Eu^{2+} ions. For SrS@Eu^{2+} only own 4f–5d Eu^{2+} excitation was detected. This differences may be referred to changes in the local environment of Eu^{2+}.

In luminescence spectra of SrS@Ce^{3+}@SrS NP a green emission with duplet at 480 and 530 nm was observed which attributed to 5d-4f Ce^{3+} electronic transitions. The duplet was originated due to spin-orbit coupling of $4f^2$ configuration of Ce^{3+}. The SrS@Ce^{3+} nanoparticles were showed only weak luminescence in region 450-600 nm which may be caused by the light emission of organic stabilizing agents on the surface of the nanoparticles.

Keywords: luminescence; surface; volume; zinc sulfides; strontium sulfide; cerium; europium.

References

[1] Shen S., Wang Q., Chem. Mater. 25 (2013) 1166.
[2] Smet Ph. F, Moreels I., Hens Z., Poelman D. Materials 3 (2012) 2834.

QUANTIFYING DEFECTS IN CARBON BASED NANOMATERIALS

J. Kalbacova[a,b*], R.D. Rodriguez[a,b], A.R. Hight Walker[c], E. Garratt[c], J.A. Fagan[c], B. Nikoobakht[c], D.R.T. Zahn[a,b]

[a] Semiconductor Physics, Technische Universität Chemnitz, 09107 Chemnitz, Germany

[b] Center of Advancing Electronics Dresden (cfaed), 09107 Chemnitz, Germany

[c] National Institute of Standards and Technology, Gaithersburg, MD 20899, USA

One of the important challenges in integrating single-wall carbon nanotubes (SWCNTs) into new applications is to be able to characterize and quantize defects. For the case of carbon based materials, Raman spectroscopy proved to be an appropriate tool to evaluate the defect concentration or the defect type.
Our aim is to investigate defects in graphite and SWCNTs induced by highly focused gallium ion beam source. The changes in the Raman spectra (D, G, G' bands) are followed with two laser excitation lines (514.7 and 632.8 nm). We show the evolution of Raman spectra with doses from $2 \cdot 10^{10}$ to 10^{15} ions/cm^2. To compare graphite to other carbon nanomaterials and its behaviour due to the irradiation, we prepared thin films of electronic type sorted – highly enriched semiconducting and metallic - SWCNTs. For all materials a pattern was created in order to statistically evaluate the role of defects.
As such, we have proven that the I_D/I_{G+} intensity ratios derived from Raman spectroscopy is quantitative measure of the defect concentration.

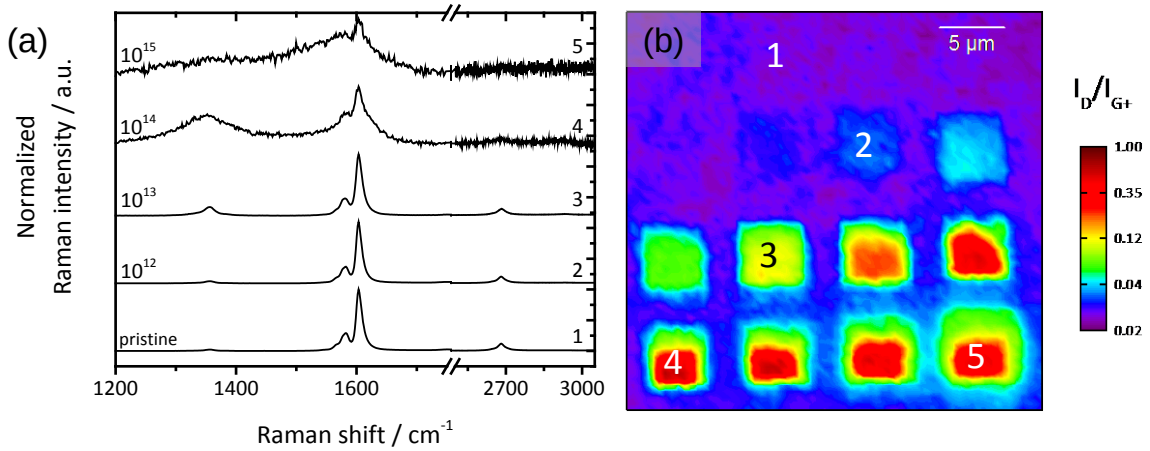

Fig. 1. Selected Raman spectra of carbon nanotubes exposed to increasing ion doses (a). 3D representation of the intensity ratio of D and G$^+$ bands (b). The ion dose is increasing from the upper left to the right and from the top to the bottom.

Keywords: graphite, carbon nanotubes, defects, Raman spectroscopy, focused ion beam

INTERCALATION OF EPITAXIAL GRAPHENE ON SiC(0001) BY ANTIMONY

S. Wolff[a], S. Roscher[a], M. Wanke[a], F. Speck[a], C. Raidel[a], M. Daniel[b], F. Timmermann[b], M. Albrecht[b], and Th. Seyller[a]

[a]Institut für Physik, TU Chemnitz, Reichenhainer Straße 70, 09126 Chemnitz, Germany
[b]Lehrstuhl für Experimentalphysik IV, Universität Augsburg, Universitätsstraße 1, 86159 Augsburg, Germany

Sublimation growth of graphene on SiC(0001) in argon atmosphere presents a well-established method for the preparation of graphene up to wafer scale [1]. This method leads to an interfacial graphene-like layer – the buffer layer (BL) – which is covalently attached to the substrate. Consequently, it lacks the electronic properties typical of graphene. The BL, however, can be detached from the SiC by intercalation, resulting in quasi-freestanding graphene. In addition, the electronic properties of graphene can be tuned by intercalation as well.

We use x-ray photoelectron spectroscopy and angle-resolved photoelectron spectroscopy to investigate intercalation of antimony, which has been predicted by theory [2]. Sb is deposited on the BL by molecular beam epitaxy. Whereas subsequent annealing in ultra-high vacuum results in re-evaporation of Sb without intercalation, Sb remains on the sample upon annealing in argon at atmospheric pressure at comparable temperatures (Fig. 1). Successful intercalation of Sb is evidenced by core-level spectroscopy, demonstrating the conversion of BL to graphene (Fig. 2).

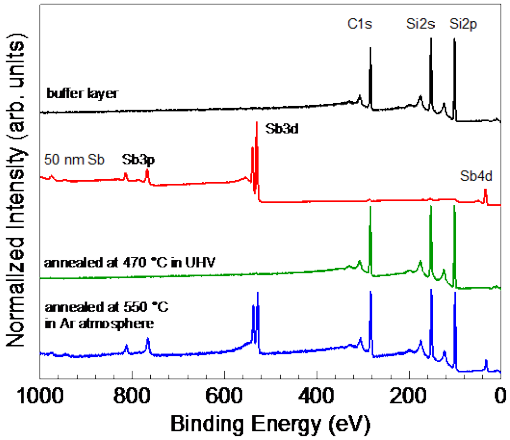

Fig. 1. Survey spectra of pristine BL, BL after deposition of 50 nm Sb, and after annealing in UHV and Ar.

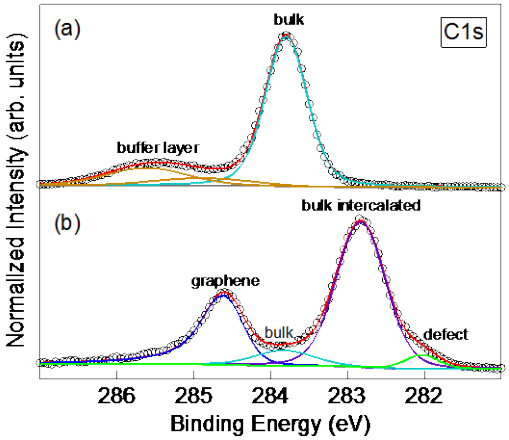

Fig. 2. C1s spectra of BL (a) before and (b) after intercalation of Sb.

Keywords: Graphene; Intercalation; Silicon carbide; Photoelectron spectroscopy

References

[1] K. V. Emtsev, A. Bostwick, K. Horn, et al., Nature Mater. 8 (2009) 203.
[2] C.-H. Hsu, W.-H. Lin, V. Ozolins, F.-C. Chuang, Appl. Phys. Lett. 100 (2012) 063115.

CHEMICAL REACTIVITY AND DOPING INVESTIGATION OF GRAPHENE WRINKLES USING RAMAN SPECTROSCOPY

Devang parmar[a], Raul D. Rodriguez[a], Tao Zhang[b], Ihsan Amin[b], Dietrich R.T. Zahn[b],

[a]Semiconductor Physics, Technische Universität Chemnitz,
Reichenhainer Str. 70, 09107 Chemnitz, Germany
[b]Makromolekulare Chemie, Technische Universität Dresden,
Mommsenstrasse 4, 01062 Dresden, Germany

Graphene is attracting much attention owing to its superior electrical, mechanical, thermal, and optical properties. Chemical vapour deposition (CVD) is a well-established method. CVD of graphene on low cost copper foil is the most prominent method for the large-scale growth of graphene. However, a particular issue of CVD graphene on copper is the presence of wrinkles. These wrinkles can contribute to the chemical reactivity and also to changes in the electronic properties of graphene. In our experiments, we have used pristine graphene prepared by CVD method on cooper and then transferred on SiO_2 substrate. Here, we investigated the chemical reactivity of basal plane and wrinkle on graphene functionalized with polystyrene bromide (PSBr). Moreover, we correlate defect concentration and doping of the different regions in graphene. For reactivity investigation, we used Raman spectroscopy and atomic force microscopy to determine the defects and structural morphology. Furthermore, we can also correlate morphology and chemical reactivity to find out how much morphology of wrinkles can affect chemical reactivity of graphene. According to our results, the wrinkles dominates the chemical reactivity of CVD graphene. Therefore, understanding the differences in chemical reactivity of wrinkles in CVD graphene could help engineering novel opto-electronic applications.

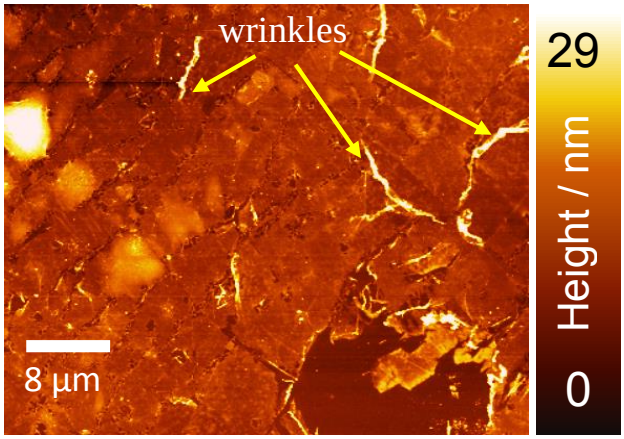

Fig. 1. Atomic force microscopy topography image of graphene functionalized with PSBr.

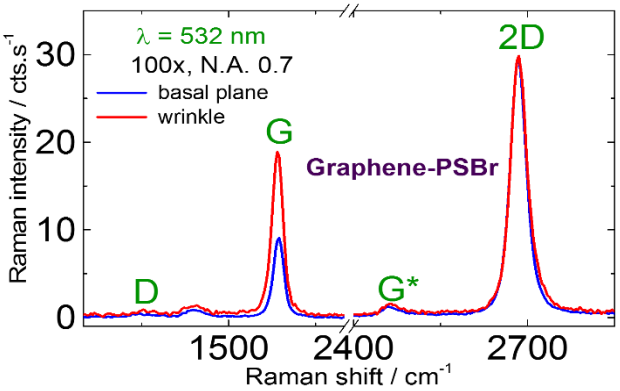

Fig. 2. Raman spectra of functionalized graphene with PSBr comparison basal and wrinkle.

Keywords: graphene, wrinkle, Raman spectroscopy, chemical vapor deposition, polystyrene bromide (PSBr)

Investigation of Defects in Graphite by Microscopic Ellipsometry

Shun Okano[a], Jana Kalbacova[a], Christoph Günther[a], Constance Schmidt[a], Elias Garratt[b], Ovidiu D. Gordan[a], Angela R. Hight Walker[c], and Dietrich R. T. Zahn[a]

[a]Semiconductor Physics, Technische Universität Chemnitz, D-09107, Chemnitz, Germany
[b]Materials Measurement Science Division, National Institute of Standards and Technology, Gaithersburg, MD 20899, USA
[c]Semiconductor and Dimensional Metrology Division, National Institute of Standards and Technology, Gaithersburg, MD 20899, USA

Carbon materials, like graphite, graphene, and carbon nanotubes, are very interesting for many technological applications. Since crystalline affect impact the physical properties, such as the refractive index and optical absorption, in this contribution we present a complementary investigation of defects in graphene by microscopic spectroscopic ellipsometry with an Accurion Nanofilm EP4 setup and micro-Raman spectroscopy and imaging. Defects were produced in square arrays of 5×5 □m^2 on highly ordered pyrolytic graphite by a focused Ga^+ ion beam. The defect concentration was varied by controlling the ion fluence from $3 \cdot 10^{10}$ to 10^{15} ions/cm. While Raman spectroscopy imaging provided information on defect concentration and changes in crystallinity and sp^2 hybridization of carbon in graphite, ellipsometry allowed determine the changes in optical properties and its correlation with defects as seen in the Δ and Ψ difference in Figures1(c) and (d), respectively. This work and the complementary approach we used contribute to the understanding of defects in carbon-based nanomaterials and their impact on optical properties.

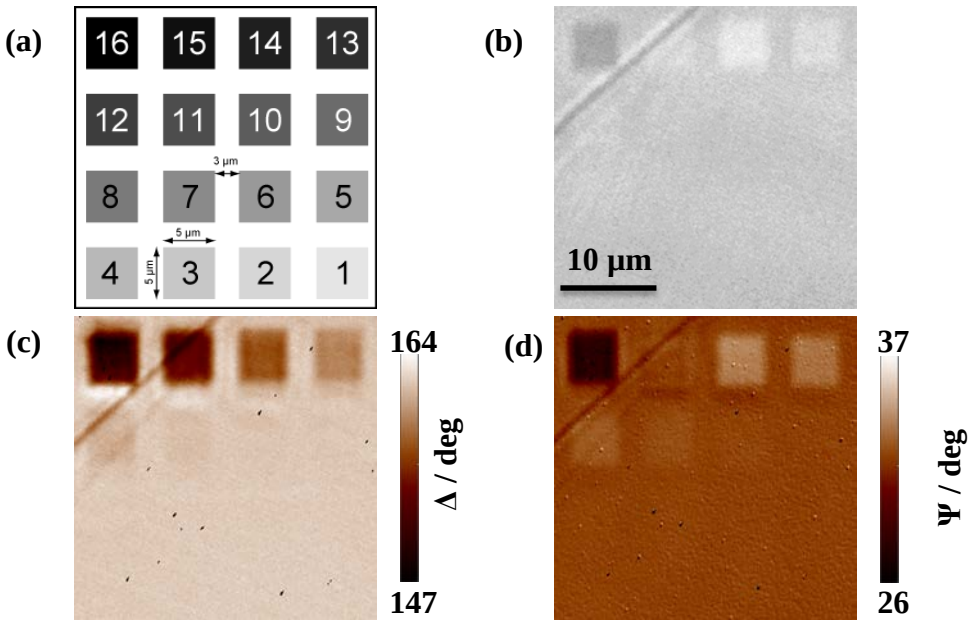

Keywords: Graphite, Micro Imaging Ellipsometry,

References

[1] G. E. Jellison et al., Physical Review B 76, 085125 (2007)
[2] Borghesi and G. Guizzetti, Handbook of optical Constants of Solids II, edited by E. D. Palik (Academic, New York, 1991)
[3] H. J. Hagemann, W. Gudat, and C. Kunz, DESY report, SR-74/7 (1974)

GROWTH AND CHARACTERIZATION OF THIN MoS_2 LAYERS ON EPITAXIAL GRAPHENE ON SiC(0001)

A. Schütze[a], M. Zeißig[a], M. Wanke[a], F. Speck[a], and Th. Seyller[a]

[a]Institut für Physik, TU Chemnitz, Reichenhainer Straße 70, 09126 Chemnitz, Germany

The unique property of layered metal dichalcogenides such as MoS_2 to transform from an indirect to a direct semiconductor when reducing the thickness to one monolayer offers new possibilities for electronic devices. For applications, however, the availability of scaleable production methods is a prerequisite.

In the present work, we investigate the chemical vapor deposition (CVD) of thin layers of MoS_2 using sulfur powder and two different molybdenum precursors, MoO_3 [1] and $MoCl_5$ [2]. MoS_2 was deposited on monolayer graphene (MLG) epitaxially grown on SiC(0001). Alternatively, the so-called buffer layer (BL), which is a graphene-like layer strongly bound to SiC(0001) [3], was used as substrate. Both BL and MLG were prepared by sublimation growth in argon at atmospheric pressure as described elsewhere [4].

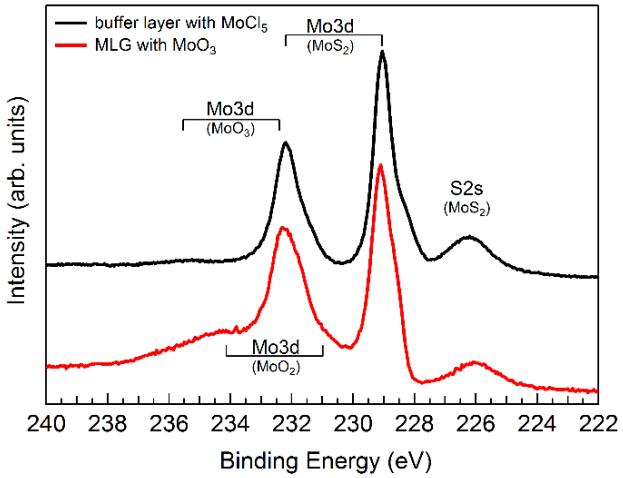

Fig. 1. Mo3d and S2s core-level spectra of CVD-MoS_2 films on buffer layer and monolayer graphene using $MoCl_5$ and MoO_3 precursors, respectively.

Samples were characterized using X-ray photoelectron spectroscopy (XPS) for the chemical composition of the samples, atomic force microscopy and low-energy electron diffraction for the structure and crystallinity of the deposited layers. For MoO_3 as precursor, a rather inhomogeneous MoS_2 growth is found which is accompanied by interface oxidation of the SiC due to oxygen intercalation. On the other hand, $MoCl_5$ as precursor results in an improved homogeneity of the deposited films and sulfur intercalation as suggested by XPS data. For the latter, a thickness of the deposited MoS_2 of approximately 1 to 3 monolayers is derived from analysis of core-level intensities.

Keywords: MoS_2; Graphene; CVD; XPS

References

[1] S. Wang et al., Chem. Mater. 26 (2014) 6371.
[2] Y. Yu et al., Sci. Rep. 3 (2013) 1866.
[3] M. Ostler et al., Phys. Status Solidi B 247 (2010) 2924.
[4] K. V. Emtsev et al., Phys. Rev. B 77 (2008) 155303.

SUBSURFACE IMAGING OF FUNCTIONALIZED AND POLYMER GRAFTED GRAPHENE OXIDE

Martin Dehnert[a], Eike-Christian Spitzner[a], Fabian Beckert[b], Christian Friedrich[b], and Robert Magerle[a]

[a]Fakultät für Naturwissenschaften, Technische Universität Chemnitz, Germany
[b]Freiburger Materialforschungszentrum, Albert-Ludwigs-Universität, D-79098 Freiburg, Germany

We investigate the surface and subsurface morphology of stearylamine modified graphene oxide sheets and polystyrene-grafted functionalized graphene oxide sheets using atomic force microscopy (AFM) operated in multiset point intermittent contact mode.[1] This allows for depth-resolved mapping of the nanomechanical properties of the top surface layer of the functionalized graphene oxide sheets.

On the surface of stearylamine functionalized graphene oxide sheets [2], we can distinguish areas of hydrophilic graphene oxide from hydrophobic areas functionalized with stearylamine. On the latter, larger repulsive forces act on the AFM tip and these areas are more deformable than the not functionalized graphene oxide surface. Measuring the height of several layers of graphene oxide and functionalized graphene oxide, we find that every single sheet of graphene oxide is functionalized with stearylamine on both sides of the sheet. The stearylamine coverage increases the bending stiffness of the stearylamine functionalized graphene oxide sheets which show no wrinkles.

Exposure of polystyrene-grafted functionalized graphene oxide [2] to chloroform vapor during the AFM measurement causes a selective swelling and a softening of the polystyrene envelope. Depth resolved mapping of the tip-sample interaction allows imaging the shape of the folded and wrinkled graphene oxide sheets within the polystyrene envelope; furthermore, it allows measuring the thickness of the swollen polystyrene envelope. This yields the swelling degree, the grafting density, and the chain conformation of the grafted polystyrene layer.

Our work demonstrates a versatile methodology for imaging and characterizing on the nanometer scale functionalized and polymer-grafted graphene oxide and other two-dimensional materials.

Keywords: Graphene oxide; surface modification; grafted polystyrene; swelling; chloroform; 3D-depth profiling; atomic force microscopy

References

[1] Spitzner, E.-C.; Riesch, C.; Szilluweit, R.; Tian, L.; Frauenrath, H.; Magerle, R., ACS Macro Lett. 1 (2012) 380.
[2] Beckert, F.; Rostas, A. M.; Thomann, R.; Weber, S.; Schleicher, E.; Friedrich, C.; Mülhaupt, R., Macromolecules 46 (2013) 5488.

DEPOPULATION OF SINGLE-PHTALOCYANINE MOLECULAR ORBITALS UPON PYRROLIC-HYDROGEN ABSTRACTION ON GRAPHENE

Nicolas Néel[a], Marie Lattelais[b], Marie-Laure Bocquet[b] and Jörg Kröger[a]

[a]Institut für Physik, TU-Ilmenau, Germany
[b]Department of Chemistry, UMR ENS-CNRS-UPMC 8640, France

Single-molecule chemistry with a scanning tunneling microscope has preponderantly been performed on metal surfaces. The molecule−metal hybridization, however, is often detrimental to genuine molecular properties and obscures their changes upon chemical reactions. We used graphene on Ir(111) to reduce the coupling between Ir(111) and adsorbed phthalocyanine molecules. By local electron injection from the tip of a scanning tunneling microscope the two pyrrolic H atoms were removed from single phthalocyanines. The detachment of the H atom pair induced a strong modification of the molecular electronic structure, albeit with no change in the adsorption geometry. Spectra and maps of the differential conductance combined with density functional calculations unveiled the entire depopulation of the highest occupied molecular orbital upon H abstraction. Occupied π states of intact molecules are proposed to be emptied via intramolecular electron transfer to dangling σ states of H-free N atoms [1].

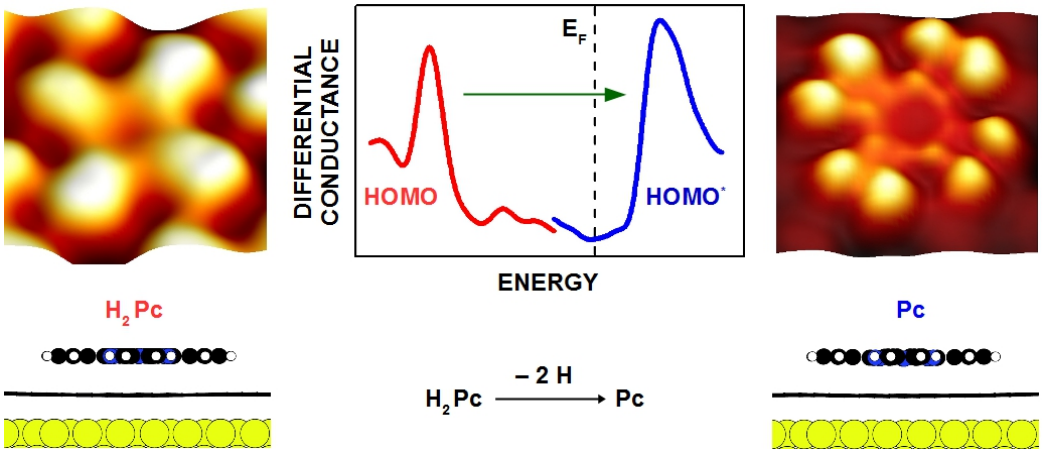

Keywords: Single molecule chemistry; Phtalocyanine; Graphene

References

[1] N. Néel, M. Lattelais, M.-L. Bocquet and J. Kröger, ACS Nanol 10 (2016) 2010.

INTERACTIONS OF TRANSITION METAL PHTHALOCYANINES AT METAL SURFACES – INFLUENCE OF INTERCALATED GRAPHENE BUFFER LAYERS

J. Uihlein[1], D. Balle[1], H. Adler[1], M. Glaser[1], M. Polek[1], T. Chassé[1] and H. Peisert[1]

[1]Inst. of Physical and Theoretical Chemistry, University of Tübingen, Tübingen (Germany)

The interactions of molecular layers with substrates strongly influence the charge transport across these interfaces, which may become important for possible future organic electronic and spintronic devices. Here, we report on investigations using X-ray absorption and photoemission spectroscopies (XAS, PES) to elucidate interactions between transition metal phthalocyanines (TMPcs) and metal substrates. In particular, the analysis of TM L-edge spectra (core-level PES and XAS) sheds light on local changes of the interface electronic structure. Valence band and TM L-edge spectra of TMPcs recorded at interfaces on Au(100) point to weak interactions only. But the spectra of the TM central atoms of TMPcs taken on Ag(111) indicate significant interactions including local charge transfer. Similar results were obtained on Ni(111), too [1]. However, for CoPc and FePc on Ni(111) the interactions can be modified by insertion of a graphene buffer-layer [2][3]. MnPc evidently reacts with the Ni(111). Graphene prevents this chemical reaction, reduces the interactions, and suppresses interfacial charge transfer [2][3]. For CoPc on graphene/Ni(111), the prevention of the charge transfer is inhibited by the strong interaction of graphene with Ni(111). This interaction can be weakened or eliminated through intercalation of copper or gold, respectively. Therefore, the disturbance of the graphene electronic structure by the interaction with the metal substrate and the corresponding charge doping has significant impact on the electronic properties of adsorbed CoPc [4].

We gratefully acknowledge cooperations by R. Ovsyannikov, and M. Bauer from Helmholtz Center Berlin, by P. Nagel, M. Merz, and S. Schuppler from ANKA/KIT, Germany, as well by A.B. Preobrajenski and A.V. Generalov, MaxLab, Sweden. We are grateful for financial support from HCB, ANKA, and MaxLab.

[1] H. Peisert, J. Uihlein, F. Petraki T. Chassé, J. Electron Spectr. Rel. Phenom. 204, 49 (2015)

[2] J. Uihlein, H. Peisert, H. Adler, M. Glaser, M. Polek, R. Ovsyannikov, T. Chassé, J. Phys. Chem. C 118 (2014) 28671

[3] J. Uihlein, H. Peisert, H. Adler, M. Glaser, M. Polek, R. Ovsyannikov, M. Bauer, T. Chassé, J. Phys. Chem. C 118 (2014) 28671

[4] J. Uihlein, M. Polek, M. Glaser, H. Adler, R. Ovsyannikov, M. Bauer, M. Ivanovic, A. Preobrajenski, A. Generalov, T. Chasse, H. Peisert, J. Phys. Chem. C 119 (2015) 15240

PHOTODEGRADATION OF PCBM AND C_{60} FILMS

A.S. Anselmo[a], P. Amsalem[b], A. Dzwilewski[c], K. Svensson[d], N. Koch[a,b] and E. Moons[d]

[a]Helmholtz-Zentrum Berlin für Materialien und Energie GmbH, Germany
[b]Institut für Physik & IRIS Adlershof, Humboldt-Universität zu Berlin, Germany
[c]Novaled AG, Germany
[d]Dept. of Engineering and Physics, Karlstad University, Sweden

Organic photovoltaics (OPV) may prove to be a competitive alternative to conventional solar cell technologies provided that there is an increase in the stability of large area devices matching what has already been achieved in terms of performance. [1] As a result of efficiency values reaching the threshold for commercial viability, interest in resolving stability and lifetime issues has increased significantly. [2]

Recent studies have focused attention on the degradation of the electron acceptor in solar cells, showing how it can impact strongly on photovoltaic performance and on the long-term integrity of the active layer. [3] Elucidating the mechanisms for degradation in fullerenes and fullerene-derivatives used in solar cells and establishing design rules for the development of more stable acceptors will contribute to increasing the general stability of the devices.

We have studied the photostability of spin-coated PCBM ([6,6]-phenyl-C61-butyric acid methyl ester) and evaporated C_{60} films using photoelectron spectroscopy (PES) and near-edge X-ray absorption fine structure (NEXAFS) spectroscopy. After exposing these materials in ambient air to simulated sunlight, the filled and empty molecular orbitals are strongly altered, indicating that the conjugated π-system of the C_{60}-cage has been compromised. [4] Studying light-exposed C_{60} films under controlled oxygen- and/or water-atmospheres will aid in elucidating the underlying mechanisms of degradation, pin-pointing the conditions under which they occur.

These results emphasize the need to control processing conditions during OPV fabrication, operation, and storage, while having important implications to the development of high throughput processing strategies.

Keywords: Degradation; Fullerene; Photostability, Photovoltaics.

References

[1] M.A. Green, K. Emery, Y. Hishikawa, W. Warta, E.D. Dunlop, Prog. Photovolt: Res. Appl. 24 (2016) 3.
[2] P. Cheng, X. Zhan, Chem. Soc. Rev. 45 (2016) 2544.
[3] M.O.Reese, A.M. Nardes, B.L. Rupert, R.E. Larsen, D.C. Olson, M.T. Lloyd, S.E. Shaheen, D.S. Ginley, G. Rumbles, N. Kopidakis, Adv. Funct. Mater. 20 (2010) 3476; A. Distler, P. Kutka, T. Sauermann, H.-J. Egelhaaf, D.M. Guldi, D.D. Nuzzo, S.C.J. Merkers, R.A.J. Janssen, J. Chem. Mater. 24 (2012) 4397; R. Hansson, C. Lindqvist, L.K.E. Ericsson, A. Opitz, E. Wang, E. Moons, Phys. Chem. Chem. Phys. 18 (2016) 11132.
[4] A.S. Anselmo, A. Dzwilewski, K. Svensson, E. Moons, Chem. Phys. Lett. 652 (2016) 220.

COATING CONTAINING MG-DOPED HYDROXYAPATITE PRODUCED BY PLASMA ELECTROLYTIC OXIDATION

C. A. Antonio[ab]; N. C. Cruz[a]; E. C. Rangel[a]; A. Delgado[c]; M. Tabacniks[d].

[a]Laboratory of Technological Plasmas, Univ. Est. Paulista, Sorocaba, Brazil
[b]Faculdade de Tecnologia de Sorocaba - FATEC-SO, Sorocaba, Brazil.
[c]Universidade Federal de São Carlos - UFSCar - Campus Sorocaba.
[d]Universidade de São Paulo – USP – Instituto de Física – São Paulo, Brazil.

The Plasma Electrolytic Oxidations (PEO) has been used to produce coatings on titanium and its alloys containing high content of HA. The PEO is an electrolytic process carried out with high voltage, in the order of hundreds of volts. The high electric field around the sample generates micro-arcs on coating surface, which produces coating with unique proprieties.

In the present study has been produced coatings on grade 4 titanium with samples of 8 mm diameter and 2 mm thick. The treatment was conducted in a tank capable of storing 1.0 L of electrolytic solution containing 0.2 M calcium acetate, 0.02 M sodium glycerophosphate and magnesium acetate with quantities variables. Between electrodes immersed in the electrolytic solution was applied to anode positive pulses of 480 V with 60% duty cycle and in the cathode, the tank itself, negative pulses of 100 V to cycles of 20% duty cicle, both at frequency of 100 Hz. The treatment time of the samples were 120 s.

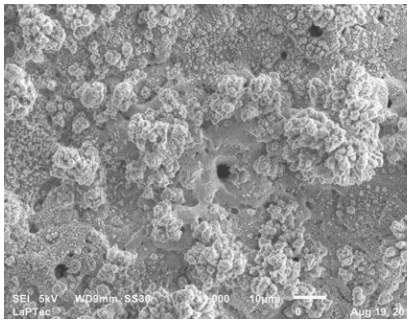

Fig. 1. Coating surface of sample with Mg-doped hydroxyapatite

The coating has been evaluated by profilometry, scanning electron microscopy and X-ray diffraction with Rietveld refinement. The coating composition was evaluated by Rutherford backscattering spectrometry and energy dispersive spectroscopy. The coatings has 50% of Mg-doped HA with incorporation of up to 3.6 a% of Mg, but larger amount of Mg in the solution has produced HA with magnesium phosphate. The effect of doping has been verified by changing the lattice parameters of the crystalline structure of the HA, where the Ca was replaced by Mg

Keywords: Plasma electrolytic Oxidations, Hydroxyapatite, Mg-doped hydroxyapatite

References

[1] A.L. Yerokhin, X. Nie, A. Leyland, A. Matthews, Surf. Coat. Technol. 130 (2000) 195 206.
[2] L. Stipniece, et al. Ceramics International 40(2014) 3261–3267.

Modifying diamond substrates by the control of surface oxygen composition.

D.A. Evans[a], Di Hu[a], S.P. Cooil[b], J.W.Wells[b]

[a]Department of Physics, Aberystwyth University, Aberystwyth SY23 3BZ, UK
[b]Department of Physics, NTNU, Trondheim, Norway

The electronic properties and reactivity of surfaces can be significantly varied by changing the nature and quantity of surface adsorbates. This is strikingly demonstrated for the low index faces of diamond where the electron affinity can be changed by several eV from negative to positive by changing the surface termination[1]. This provides a route for engineering surfaces and interfaces for electron emission, electron transport and chemical sensors.

Here, we report a protocol for the oxidation of diamond surfaces and the controlled replacement of oxygen by hydrogen. The latter process has been continuously monitored by real-time electron spectroscopy as illustrated for the O1s core level emission in Figure 1. The fully oxygen-terminated surface at 23ºC is stable up to a temperature of 350ºC (region 1). Above this temperature, the oxygen desorbs rapidly (region 2) and is eventually replaced by hydrogen.

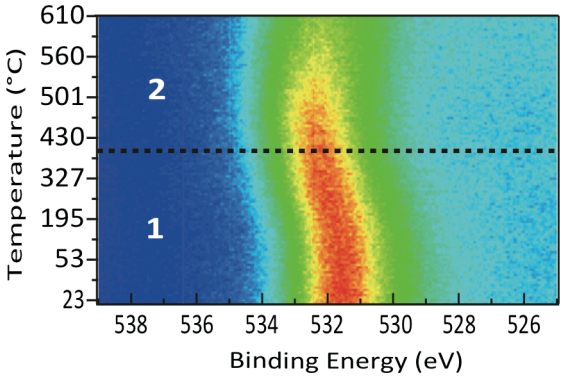

Fig. 1. O1s core level evolution during thermal desorption of oxygen from the diamond (001) surface

Variations in the energy positions of key features in the photo-electron distribution enable compositional changes to be correlated with the electronic structure and chemical reactivity[2]. Control of the surface conductivity is illustrated by adsorbing small molecules on differently prepared diamond surfaces and control of the surface reactivity is illustrated by the interaction of diamond with volatile cancer treatment drug molecules.

Keywords: surfaces; diamond; adsorbates

References

[1] J. B. Cui, J. Ristein, L. Ley, *Phys. Rev. Lett.* **1998**, *81*, 429-432.
[2] G. T. Williams, S. P. Cooil, O. R. Roberts, S. Evans, D. P. Langstaff, D. A. Evans, *Applied Physics Letters* **2014**, *105*, 061602.

IN-SITU STUDY OF THE FIRST STEP'S OF COPPER OXIDE FORMATION ON Cu (110) ELECTRODE SURFACE

Reza Sharif[a], Jiri Duchoslav[b], Miao-Hsuan Chien[a], Saul Vazquez Miranda[a], Kurt Hingerl[a], and Christoph Cobet[a]

[a]Center for Surface- and Nanoanalytics (ZONA), Johannes Kepler University Linz, Altenberger Straße 69, A-4040 Linz, Austria
[b]Christian Doppler Laboratory for Microscopic and Spectroscopic Material Characterization, Center for Surface and Nanoanalytics, Johannes Kepler University Linz, Altenberger Straße 69, A-4040 Linz, Austria

Copper corrosion and oxidation as well as oxygen adsorption process on single crystal copper surface in UHV has been studied systematically [1], However, due to the complexity of the solid-liquid interface [2], the mechanism of the first steps of copper oxide formation in electrochemical environment are not completely understood.

In this work, we study the anodic oxidation of Cu (110) single crystal in 3mM $HClO_4$, PH< 3 acidic solution with Cyclic Voltammetry (CV), in which the integrated charge and ion-exchange is measured. Additionally, we used highly surface-sensitive in-situ Reflection Anisotropy Spectros-copy (RAS) to monitor the reaction processes based on the specific optical respond of the oxide adlayer. The composition of the layers has also been studied qualitatively and quantitatively with chemical and surface analytical methods such as X-ray photoelectron spectroscopy (XPS) at emersed sample. As shown in the CV (Fig.1.), oxide adsorption/desorption peaks are present around -550mv/-600mv. The oxidation was then investigated by comparing the XPS measurement at two defined potentials: one before -550mv and another after -550mv, referring to the pristine Cu metal and copper surface after first oxidation step, respectively. The transition of Cu metal to Cu(I) as a Cu_2O formation is confirmed, with the absence of Cu(II). Our first results provide already additional insight into the oxidation of Cu(110) in acidic electrochemical environment.

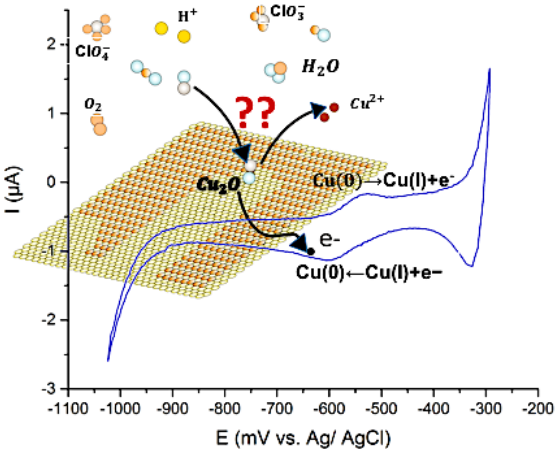

Figure 1. Copper oxide formation on Cu (110) Electrodes in 3mM $HClO_4$

Keywords: Cu (110), XPS, RAS, CV, oxidation, electrochemistry.

References

[1] L.D. Sun, P. Zeppenfeld. et al., Surface Science 602 (2008) L1–L4.
[2] G. Barati, C. Cobet, et al., Langmuir 30 (2014) 14486–14493.

CORROSSION RESISTANCE OF CARBON STEEL COATED WITH A SiO_X-ORGANOSILICON LAYER

R.C.C. Rangel[a], E.C. Rangel[a], N.C. Cruz[a], F. Fanelli[b], F. Fracassi[b].

[a]Technological Plasma Laboratory, Paulista State University - UNESP, Science and Technology Faculty, Sorocaba, SP, Brazil
[b]Department of Chemistry, University of Bari Aldo Moro, Bari, Italy

Carbon steel is the most commonly used material for sheets, plates, bars and tubes in mechanical metallurgy and construction industry. However, the susceptibility of carbon steel to oxidation under real conditions of use turns preventive and corrective repairs mandatory. A way to avoid this phenomenon is to coat the metal with a layer, which inhibits permeation of corrosive agents to the metal interface. Some works suggest the development of protective coatings using the plasma deposition technique based on hexamethyldisiloxane, HMDSO, compound. Altering the plasma excitation parameters, enables to deposit organosilicon ($SiO_xC_yH_z$) to oxide (SiO_x) films. Literature works use this flexibility to prepare multilayered films. However most of these works does not study the interference of the order of the layers application on the corrosion resistance of the system. Considering that, the present work aims to study the corrosion resistance of the carbon steel coated with multilayers constituted of SiO_x and $SiO_xC_yH_z$ films in different sequences. SiO_x-organosilicon multilayers were deposited by low pressure radiofrequency (13.56 MHz) plasmas using HMDSO, Ar and O_2 mixtures. The change of an organosilicon to inorganic coating or vice versa was made only by adjusting the plasma conditions without interrupting the process. It was investigated what sequence of monolayers leads to better barrier properties. Electrochemical Impedance Spectroscopy, EIS, and potentiodynamic polarization were used to evaluate the corrosion resistance provided by the multilayer to the carbon steel. Infrared spectroscopy, FTIR, was applied to analyze the chemical composition and molecular structure of the layers. The thickness of the films was measured by profilometry while the morphology and roughness were determined by atomic force microscopy, AFM. The surface wettability was evaluated by contact angle measurements. The best results of corrosion resistance, R_t, of the multilayer system have been obtained with an outermost organosilicon layer. The coating of carbon steel with the multilayered film resulted in an increase of 6 orders of magnitude in R_t.

Keywords: Carbon steel; Corrosion resistance; SiO_x-organosilicon multilayers; Plasma

The authors want to thank FAPESP (São Paulo State Research Foundation) for financial support.

SURFACE TRANSPORT ON THIN SEMI-METALLIC FILMS: THE ROLE OF FILM THICKNESS AND MAGNETIC IMPURITIES

P. Kröger[a], M. Siemens, C. Tegenkamp[a], H. Pfnür[a]
[a]Institut für Festkörperphysik, Leibniz Universität Hannover, Germany

The semi-metal bismuth has attracted a lot of interest because of its unique electronic properties such as low carrier concentrations and high carrier mobilities. Thereby, epitaxial growth of high-quality thin films opens new pathways to tailor the electronic properties further, e.g. by quantum confinement [1] and alloy formation [2], giving rise to topologically non-trivial states in this material class. In this study we concentrate on Bi films grown on Si(111). Thin Bi(111) films become semiconducting, thus the peculiar spin texture of the surface states, induced by the Rashba effect, can be studied directly by temperature and magnetic field dependent transport.
The conductance G at low temperature is mainly governed by surface states while at higher temperatures activated transport from bulk channels sets it. We have carefully analyzed the G(T)-behaviour for variously thick films. With decreasing film thickness, the bulk gap increases, as expected due to the quantum size effect. However for thinner films the gap decreases and finally the surface states overlap with bulk bands. The reason is an interface-interface interaction which renormalizes strongly the Fermi surfaces [1].
Moreover, magnetic impurities Cr, Co, Fe and Mn, in the range of a few percent of a monolayer were added to probe the scattering behavior of the spin-polarized surface channels by magneto-conductance. The adsorption of all of these elements is accompanied by charge transfer (0.3-0.5h/atom) and strong spin-orbit scattering, which results in a transition of strong weak anti-localization to weak localization. The strength of spin orbit scattering differs among the magnetic atoms and is directly connected to their magnetic moment in the adsorbed state [3].

*Keywords:*semi-metallic films, surface transport, magnetic impurities

References

[1] T. Hirahara et al.PRL 115, 106803 (2015)
[2] J. Koch, P. Kröger, H. Pfnür, C. Tegenkamp, „Surface state conductivity in epitaxially grown $Bi_{1-x}Sb_x$ films", submitted
[3] P. Kröger, S. Sologub, C. Tegenkamp, H. Pfnür, JPCM 26, 225002 (2014).

OPTICAL PROPERTIES OF SELF-ORGANIZED NANOSTRUCTURED HYBRIDE FILMS DOPED BY RHODAMINE 6G

A. Bogoslovskaya[a], E. Bortchagovsky[a], E. Leonenko[b] and G. Telbiz[b]

[a]V.E. Lashkaryov Institute of Semiconductor Physics of NAS of Ukraine, pr.Nauki 41, Kyiv 02028, Ukraine
[b]L.V. Pisarzhevskii Institute of Physical Chemistry of NAS of Ukraine, pr.Nauki 31, Kyiv 03028, Ukraine

Nanostructured SiO_2 and TiO_2 films were prepared via the template sol-gel pre-doping technique using tetraethoxysilane or titanium isopropoxide as precursor material and Pluronic 123 as surfactant. Dye Rhodamine 6G in different concentration was used as the dopant. It was demonstrated that the method of deposition as well as the condensation rate of the precursor and the evaporation of the solvent reflects in the resulting complexation of the dye. The ability of the occluded Pluronic P123 mesostructures to solubilize organic molecules made these films ideal host matrices for organic dyes and molecular assemblies.

The scheme of the self-organization of the resulting film is shown in Fig.1. Creation of such a columnar structure is directly confirmed by the results of ellipsometric measurements.

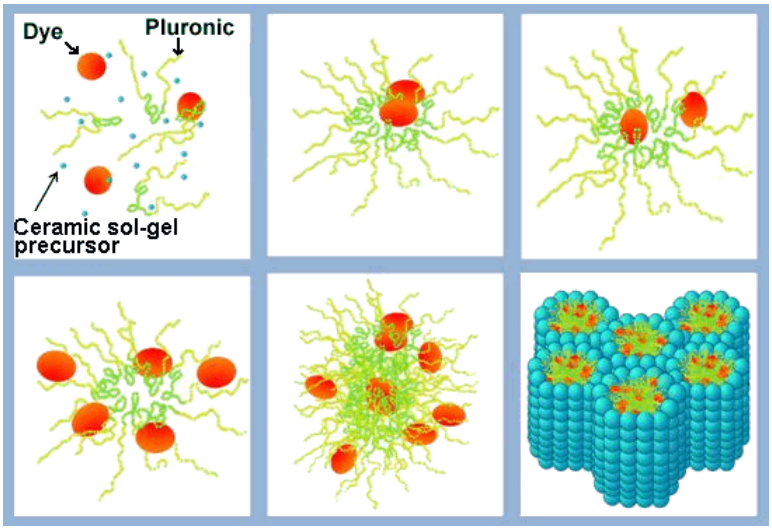

Fig. 1.Self-organization of the film structure

Different approaches to the preparation of such a films allow to manage the complexation and optical properties of organic dyes impregnated into the nanoporous silica skeleton. Controlling the Pluronic P123 concentration we are able to control the aggregation of Rhodamine molecules and in such a way to manage fluorescent properties of resulted films [1]. Additionally, optical properties are affected by the geometrical restriction of the aggregation and complexation of organic dyes by the structure of nanoporous silica skeleton. It was demonstrated earlier, that such films have high nonlinear properties and the potential in the use as the photonic layer in an all-optical switching device [2].

Keywords: Rodamine 6G, self-organization, fluorescence, ellipsometry

References

[1] E. V. Leonenko, G. M. Telbiz, A. B. Bogoslovskaya, and P. A. Manoryk; Theor. Experiment. Chem.; **50** (2015) 358-363.
[2] G. Telbiz, S. Bugaychuk, E. Leonenko, L. Derzhypolska, V. Gnatovskyy, and I. Pryadko; Nanoscale Res. Lett.; **10** (2015) 196-1-7.

SELECTIVE NUCLEATION OF MnSb ISLANDS ON GaAs SUBSTRATES

C. Klump[1], C. Godde[1], S. Noor[1], J. Ritzmann[2], A. Ludwig[2], A. Wieck[2], and U. Köhler[1]

[1]Experimentalphysik IV, AG Oberflächen, Ruhr-Universität Bochum, Germany
[2]Lehrstuhl für Angewandte Festkörperphysik, Ruhr-Universität Bochum, Germany

For future spintronic semiconductor devices, spin polarization and injection is one important prerequisite. Ferromagnetic or half-metallic materials are one possible approach for efficient spin-injectors. As with the underlying semiconductor quantum dots, it is necessary to be able to grow the spin-injector material site-selectively in order to build well-defined quantum devices. For site-selective growth of semiconductor quantum dots, two methods were mainly used, which use substrate pre-structuring and surface strain as driving force, respectively. These methods can be transferred to spin-injector materials.
Prestructuring the substrates introduces defects to the surface and may deteriorate the quality of subsequent island growth, which will influence the magnetic properties and lower the spin polarization efficiency. Examples of growth on a prestructured substrate are shown.
Strain-driven nucleation, on the other hand, opens the prospect of pin-pointing exactly one spin-injector island to one semiconductor QD by using the inherent strain induced by the underlying semiconductor QD, so spin-injection can be studied for each QD, individually.
MnSb is an interesting material for spin-injection with its high Curie temperature of 587 K and its compatibility with semiconductor substrates. The strain induced pairing of MnSb islands with InAs QDs is studied. As a first step, structural properties, such as island density and size, have to be matched with the underlying pattern of semiconductor QDs. MnSb islands were grown on different GaAs substrates by MBE. Structural and magnetic properties have been studied by STM, LEED and MOKE.

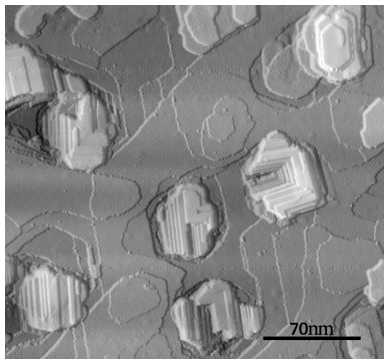

Fig. 1. Example of site-selective growth driven by prestructured substrate. Nucleation of Sb-islands in etch-pits of the GaAs substrate.

Keywords: magnetic nanostructures; Quantum dots; self organized nucleation; GaAs

RAMAN SPECTROSCOPY OF THE LATTICE DYNAMICS AND CRYSTAL FIELD SPLITTING IN $CePt_5$ LAYERS ON Pt(111)

B. Halbig[a], U. Bass[a], J. Geurts[a], M. Zinner[b] and K. Fauth[b]

[a]Physikalisches Institut, Exp. Physik 3, Universität Würzburg, Germany
[b]Physikalisches Institut, Exp. Physik 2, Universität Würzburg, Germany

Ultrathin layers of the binary intermetallic compound $CePt_5$ with thicknesses of few unit cells have found great interest in the field of Kondo physics, originating from the interaction of the localized Ce $4f^1$ electrons with the itinerant electrons [1]. Such $CePt_5$ layers are generated on Pt(111) surfaces in UHV by deposition of elemental Ce and subsequent annealing, resulting in a hexagonal crystalline $CePt_5$ structure, which consists of alternating $CePt_2$ and Pt atomic layers (the latter forming a kagome lattice), and is terminated at the surface by a dense hexagonal Pt layer [2,3]. In this crystal structure a splitting of the Ce 4f electron levels by the crystal electric fields of the neighboring Pt atoms is expected to enable transitions of the 4f electron in the meV range. These transitions should be observable in Raman spectroscopy. Furthermore, the $CePt_5$-layer should give rise to phononic Raman scattering from the lattice.

We report on the determination of the crystal-field-induced 4f level splitting in $CePt_5$ layers with thicknesses between 3.5 and 18 unit cells on Pt(111) surfaces by electronic Raman spectroscopy from crystal field excitations (CFE). For reference we used identically prepared $LaPt_5$ layers, i.e., with the same crystal structure, but without 4f electrons.

In the Raman spectra of $CePt_5$ at $T \approx 20$ K three distinct peaks appear, which are absent for $LaPt_5$. The Raman shifts of these $CePt_5$ peaks range from approximately 15 meV to about 25 meV. Based on the individual dependence of their intensities on the layer thickness, we assign these three peaks to CFE of Ce 4f electrons, located (i) in the $CePt_5$ layer, (ii) at the interface of the $CePt_5$ layer to the Pt(111) substrate, and (iii) at the Pt-terminated surface of the $CePt_5$ layer, respectively.

Besides, up to three additional sharp Raman peaks occur in an almost identical pattern both for $CePt_5$ and for $LaPt_5$. Therefore they are identified as crystal lattice vibrations. For the case of $CePt_5$, one of them is assigned to the $CePt_5$ E_{2g} mode, whose symmetry corresponds to the CFE, the others to vibrations of the uppermost part of the $CePt_5$ layer, which is symmetry-reduced due to surface relaxation [3].

Keywords: Raman; $CePt_5$; Crystal Field Excitations

References

[1] C. Praetorius *et al.*, Phys. Rev. B 92 (2015) 045116
[2] J. Kemmer *et al.*, Phys. Rev. B 90 (2014) 195401
[3] C. Praetorius *et al.*, Phys. Rev. B 92 (2015) 195427

MAGNETISN OF Fe3Si FILMS AND ITS CORRELATION WITH ITS CRYSTALLOGRAPHIC PROPERTIES

I.Arnay[a], J. Rubio-Zuazo[a], J. López-Sánchez[b], G. R. Castro[a]

[a]BM25-SpLine, ESRF (European Synchrotron Radiation Facility), 71 Avenue Martyrs, 38000 Grenoble, France
[a]ICMM-CSIC (Instituto de Ciencia de Materiales de Madrid), Ciudad Universitaria de Cantoblanco, 28049 Madrid, Spain
[b]Departamento de Física de Materiales, Facultad de Ciencias Físicas, Universidad Complutense de Madrid, Ciudad Universitaria s/n, 28040 Madrid, Spain
[b]Unidad Asociada IQFR (CSIC)-UCM, 28040 Madrid, Spain

The increasing interest in spintronic have motivated the study and development of new ferromagnetic films. Fe3Si is a good candidate as a ferromagnetic electrode due to its high spin polarization and high Curie temperature [1]. Moreover, Fe3Si presents larger resistance when compared to conventional ferromagnets as Fe or Co, which have been proposed as a possible solution for the impedance-mismatch problem in the spin injection through ferromagnet/semiconductor barriers [2, 3]. It is found that the spin-polarized conductance and bias-dependent TMR ratios are rather sensitive to the structure of the Fe3Si electrode. Theoretical studies suggests that there is no spin-polarization for the cubic Fe3Si while, in contrast, the tetragonal Fe3Si presents half-metal nature [4]. Growing thin films allow us to manipulate the structural characteristic of the electrode.

In this context we have prepared by PLD a set of four samples with different crystallographic structure. Fe3Si was evaporated on MgO, STO, LaAlO3 and SiO2/Si getting different crystallographic properties. Clear different magnetic response was obtenied as a function of the crystalograpic behaviour as shown in Fig 1. In this work we will present a complete characterization of the crystallographic structure, elemental composition and magnetism of the samples by RHEED, synchrotron radiation-XRD, XPS and MOKE.

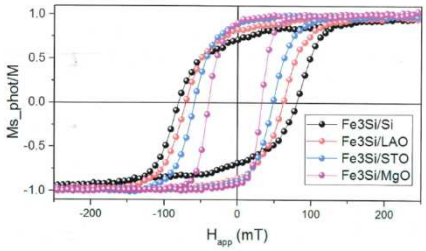

Fig.1: In-plane magnetic hysteresis loops

Keywords: Magnetism; Spintronics

References

[1] A.Ionescu, C. A. F. Vaz, T. Trypiniotis, C. M.Gurtler, H. García-Miguel, J. A. C. Bland, M. E. Vickers, R. M. Dalgliesh, S. Langridge, Y. Bugoslavsky, Y. Miyoshi, L. F. Cohen, and K. R. A. Ziebeck, Phys. Rev. B **71**, 094401 (2005)
[2] G. Schmidt, D. Ferrand, and L. W. Molenkamp, Phys. Rev. B **62**, R4790(R) (2000)
[3] E. I. Rashba, Phys. Rev. B **62**, R16267 (2000)
[4] L. L. Tao, S. H. Liang, D. P. Liu, H. X. Wei, J.Wang, and X. F. Han, Appl. Phys. Lett. **104**, 172406 (2014)

Structure and bonding control in ultrathin iron films

Di Hu[a], S.P. Cooil[b], A. Zakharov[c], C. Feng[d], D.A. Evans[a]

[a]Department of Physics, Aberystwyth University, Aberystwyth, UK
[b]Department of Physics, NTNU, Trondheim, Norway
[c]MAXLab, Lund, Sweden
[d]Department of Materials Physics and Chemistry, University of Science and Technology, Beijing, China

Thin films of transition metals such as iron can exhibit different structural, electronic and magnetic properties when grown on different substrates and with different thickness[1]. The highest structural quality requires a close epitaxial match with the substrate and control of the growth parameters.

Here we demonstrate the growth of thin films of iron on epitaxially-matched, single-crystal substrates and non-matched polycrystalline metal substrates, monitored in-situ using laboratory-based and synchtroron-based electron methods (Photolectron Spectroscopy (XPS, UPS), Photoelectron Microscopy (PEEM Electron Diffraction (LEED, LEEM).

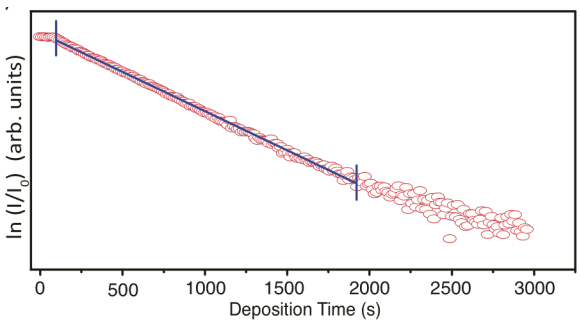

Fig. 1. Real-time monitoring of substrate photoelectron emission during MBE growth of iron.

Epitaxial iron films grown on lattice-matched substrates exhibit 2d growth as shown in the real-time photoelectron emission data presented in Fig. 1. The substrate in this example was a single-crystal diamond, with (111) surface orientation[2]. The C1s core level emission intensity was found to decrease exponentially during film growth, and was fully attenuated by a film of thickness 10 nm. On annealing in vacuum, the FCC iron film exhibited a phase transition to BCC as revealed in LEED and LEEM. Even on non-lattice matched substrates, a change in lattice constant of the iron films was determined from the change in binding energy of the thin film core level states. This was found to correlate with changes in the electronic and magnetic properties of the film.

Keywords: thin films; iron; photoemission

References

[1] W. Daum, C. Stuhlmann, H. Ibach, *Phys. Rev. Lett.* **1988**, *60*, 2741-2744.
[2] S. P. Cooil, F. Song, G. T. Williams, O. R. Roberts, D. P. Langstaff, B. Jorgensen, K. Hoydalsvik, D. W. Breiby, E. Wahlström, D. A. Evans, J. W. Wells, *Carbon* **2012**, *50*, 5099-5105.

SURFACE DYNAMICS OF 0.5-1 ML Pb on Cu(111)

I.Yu. Sklyadneva[a], G.G. Rusina[b,c], S.D. Borisova[b,c], S.V. Eremeev[b,c], E.V. Chulkov[a], G. Benedek[d], J.P. Tiennies[e]

[a] Donostia International Physics Center (DIPC), 20018 San Sebastián, Spain
[b] Institute of Strength Physics and Materials Science, 634021, Tomsk, Russia
[c] Tomsk State University, 634050 Tomsk, Russia
[d] Universitá di Milano-Bicocca, 20125 Milano, Italy
[e] Max-Planck-Institut für Dynamik und Selbstorganisation, Göttingen, Germany

Thin metal films on metal surfaces are of great interest as model systems for materials with reduced dimensionality. For ultra-thin Pb films on Cu(111) it was demonstrated that the HAS inelastic intensities provide a direct measurement of mode-selected electron-phonon (*e- ph*) coupling strengths for individual surface and sub-surface phonons (mode-lambda spectroscopy) [1], thus allowing to assess which phonons are actually relevant in superconductivity. For a correct description of the distribution of the phonon density of states in the film, it is important to take into account the emerging structure of the interface and the interaction between the film atoms and the atoms of the first substrate layer. The calculations presented here are based on the embedded atom method (EAM) and include the dynamics of the substrate (Fig.1). Besides leading to a detailed interpretation of the HAS experimental data, the present results are compared with a density-functional perturbation theory study on a *rigid* substrate. The comparison reveals the role played by the substrate dynamics at the smallest thicknesses, despite the large mass and stiffness differences between Pb and Cu.

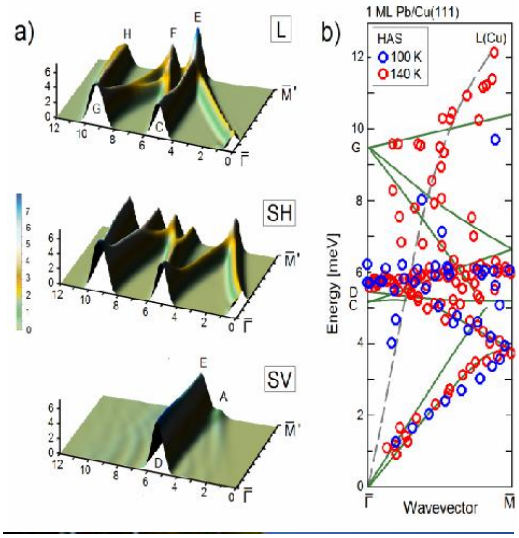

Fig.1. (a) Wave-resolved phonon density and (b) phonon dispersion

The EAM structure analysis also reveals a considerable corrugation of the film surface and of the substrate atomic layers. A dynamically stable structure is formed with a low-energy stretching mode which results from a strong coupling of the monolayer phonons with the low-energy shear-vertical vibrations of the top substrate atoms.

Keywords: Superconducting films, interfaces and surfaces

References

[1] G. Benedek, M. Bernasconi, K.-P. Bohnen, D. Campi, E.V. Chulkov, P.M. Echenique, R. Heid, I.Yu. Sklyadneva, J.P. Toennies, Phys. Chem. Chem. Phys.**16** (2014) 7159.

PHOTOTHERMAL AND VIBRATIONAL MAPPING OF SURFACES AND INTERFACES BEYOND THE DIFFRACTION LIMIT OF LIGHT

Adarsh Reddy[a], Raul D. Rodriguez[a], Rayhan Rasel[a], Zoheb Khan[a], Teresa I. Madeira[b], Harsha Shah[a], Eugene Bortchagovsky[c], and Dietrich R.T. Zahn[a]

[a]Semiconductor Physics, Technische Universität Chemnitz, D-09107 Chemnitz, Germany.
[b]BioISI – Biosystems & Integrative Sciences Institute, Faculdade de Ciências da Universidade de Lisboa, Campo Grande, C8, 1749-016 Lisboa, Portugal
[c]Institute of Semiconductor Physics of NASU, pr.Nauki 41, Kiev 03028, Ukraine

The diffraction limit of light was regarded as a fundamental unbreakable barrier that prevented the visualization of objects with size smaller than half the light wavelength, until super resolution optical methods and near-field optics allowed overcoming that constraint [1,2]. We report on a new approach based on tracking the photo-thermal expansion (nano-vis) in combination with tip-enhanced Raman spectroscopy (TERS). A commercial TERS system based on atomic force microscopy is coupled to a mechanical switch for intermittent visible light excitation. This simple configuration allows detecting small changes in the nano-object volume. Contrary to nano-IR that is based on the detection of molecular and lattice vibrations [3], the principle behind nano-vis involves tracking the heat generated from electronic transitions and scattering during the relaxation in the sample material that occurs due to optical absorption in the visible spectral range. The sensitivity and spatial resolution are further improved by the combined effect of electric field enhancement obtained by excitation of localized surface plasmons, and the synchronization of mechanical resonance of the tip-cantilever system with the intermittent light excitation. Our concept is demonstrated by the TERS and nano-vis analysis of a two-dimensional material (GaSe) on graphite and by an array of multi-walled carbon nanotubes lithographically designed in a silicon oxide matrix. In addition to TERS, an unprecedented spatial resolution for optical absorption below 10 nm is reported.

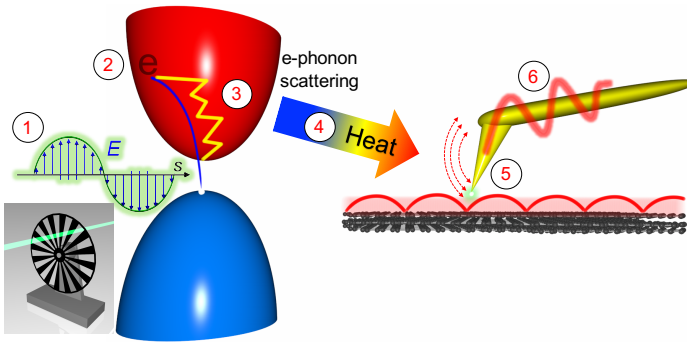

Figure 1: (a) Physical schematics behind nano-vis: (1) a chopper allows the intermittent passage of photons with energy high enough to excite an electron from the valence band to a high energy level (2) in the conduction band, non-radiative relaxation (3) mediated by e-phonon scattering induces (4) heat increase that results in the thermal expansion of the sample (5) and the cantilever deflection (6).

Keywords: nano-optics, photo-thermal imaging, tip-enhanced Raman spectroscopy, TERS, plasmonics, atomic force microscopy

References

[1] Langelüddecke, L., Singh, P. & Deckert, V. Applied spectroscopy69, 1357-1371 (2015).
[2] Katzenmeyer, A. M., Holland, G., Kjoller, K. & Centrone, A. Analytical Chemistry 87, 3154-3159, doi:10.1021/ac504672t (2015).
[3] Dazzi, A., Prazeres, R., Glotin, F. & Ortega, J. Optics letters30, 2388-2390 (2005)

THE ROLE OF TIP-SAMPLE INTERACTION IN TIP-ENHANCED RAMAN SPECTROSCOPY IMAGING

Hassan Banayeem[a], Raul D. Rodriguez[b,c], Evgeniya Sheremet[a], Anurag Adiraju[b], Michael Hietschold[a], Dietrich R.T. Zahn[b,c]

[a]Solid Surfaces Analysis Group, Technische Universität Chemnitz, 09107 Chemnitz, Germany
[b]Semiconductor Physics, Technische Universität Chemnitz, 09107 Chemnitz, Germany
[c]Center for Advancing Electronics Dresden (cfaed), Technische Universität Chemnitz, 09107, Chemnitz, Germany

The capability to visualize and correlate composition, sample properties, and morphology with a resolution at the nanoscale makes tip-enhanced Raman spectroscopy (TERS) one of the hottest topics in nanoscale characterization since first reported in 2000 [1-3]. Numerical models and previous experimental results showed that the electric field enhancement in TERS is a direct consequence of tip-sample geometry, composition, and laser excitation [4]. In this contribution we show that in addition to those parameters, the tip-sample interaction makes also an impact in image contrast of TERS. Numerical simulations and experimental results show that the attractive tip-sample interaction results in a larger increase of electric field enhancement that is related to an optimal tip-sample distance in that interaction regime. We demonstrate how and why the tip-sample interaction must be considered in the interpretation of TERS imaging results obtained with dynamic mode AFM. These results can be generalized, with implications in other scanning probe based nano-optical methods such as scanning near-field optics (SNOM) with a tuning fork.

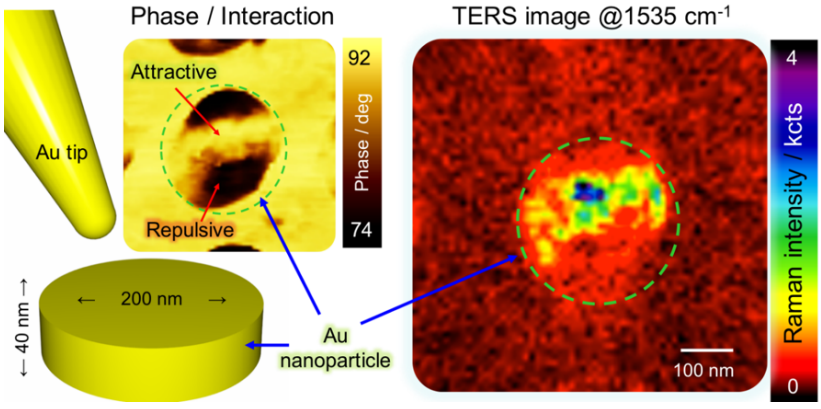

Figure 1: Phase contrast comparison for AFM imaging of a gold nanoparticle with a gold cantilever-tip [5]. The phase image correlation with TERS image contrast obtained under 638 nm excitation, the Raman probe was a 2 nm film of CoPc. The TERS image shows the spatial distribution of the B_{1g} mode intensity of CoPc at 1535 cm^{-1}. Both images were obtained simultaneously.

Keywords: tip-enhanced Raman spectroscopy, TERS, atomic force microscopy, plasmonics

References

[1] R.M. Stockle, Y.D. Suh, V. Deckert, R. Zenobi, Chemical Physics Letters, 318 (2000) 131-136.
[2] N. Hayazawa, Y. Inouye, Z. Sekkat, S. Kawata, Optical Communications, 183 (2000) 333-336.
[3] M.S. Anderson, Applied Physics Letters, 76 (2000) 3130-3132.
[4] Z.L. Yang, J. Aizpurua, H.X. Xu, Journal of Raman Spectroscopy, 40 (2009) 1343-1348.
[5] E. Sheremet, R. D. Rodriguez, A. L. Agapov, A. P. Sokolov, M. Hietschold, and D. R. T. Zahn, Carbon, 96, (2016), 588-593.

Ab initio calculations and infrared plasmonic investigation of metallic properties of the Si(111)-(5x2)-Au surface

Kaori Seino[a], Fabian Hötzel[b], Annemarie Pucci[b], Friedhelm Bechstedt[c], Simone Sanna[a] and Wolf Gero Schmidt[a]

[a]Lehrstuhl für Theoretische Physik, Universität Paderborn, Paderborn, Germany
[b]Kirchhoff Institute for Physics, Heidelberg University, Heidelberg, Germany
[c]Institut für Festkörpertheorie und -optik, Friedrich-Schiller-Universität Jena, Jena, Germany

Self-assembled atomic wires fabricated on semiconductor surfaces are promising candidates for future nanoelectronics. The Si(111)-(5x2)-Au surface is one of the examples where atomic nanowires appear. For a long time it has been the subject of experimental and theoretical studies. After the revision of the Au coverage to be 0.6 monolayer (ML) [1], new atomic models have been proposed and discussed [2-4]. Erwin *et al.* proposed a model consisting of a gold single row, a gold double row, and a silicon honeycomb chain (EBH model) [2], corresponding to an Au coverage of 0.6 ML. Later, Kwon and Kang proposed a model containing an additional Au atom per (5x2) unit cell (KK model) [3], corresponding to an Au coverage of 0.7 ML. The KK model is energetically favored than the EBH model for rather Au-rich preparation conditions.

The metallic character down to 20 K and the KK model with 0.7 ML Au coverage of the Si(111)-(5x2)-Au surface are confirmed by infrared spectroscopy [5]. Relative transmittance spectra show a broad, anisotropic absorption signal which is attributed to a localized surface plasmon forming a standing wave due to the finite lengths of the wires. The spectral line shape is analyzed quantitatively by a quasistatic absorption cross section which yields important band structure related information. Upon the evaporation of an additional submonolayer amount of gold, the surface becomes insulating but keeps the 5x2 symmetry. This metal-to-insulator transition was in situ monitored based on the infrared plasmonic signal change with coverage [6]. The phase transition is theoretically explained by total-energy and band-structure calculations for a novel structural model.

Keywords: Metallic nanowires; Semiconductor surfaces; Density functional theory; Plasmon

References

[1] I. Barke, F. Zheng, S. Bockenhauer, K. Sell, V. Oeynhausen, K. Meiwes-Broer, S. Erwin, and F. Himpsel, Phys. Rev. B 79 (2009) 155301.
[2] S. C. Erwin, I. Barke, and F. J. Himpsel, Phys. Rev. B 80 (2009) 155409.
[3] S. G. Kwon and M. H. Kang, Phys. Rev. Lett. 113 (2014) 086101.
[4] K. Seino and F. Bechstedt, Phys. Rev. B 90 (2014) 165407.
[5] F. Hötzel, K. Seino, C. Huck, O. Skibbe, F. Bechstedt, and A. Pucci, Nano Lett. 15 (2015) 4155.
[6] F. Hötzel, K. Seino, S. Chandola, E. Speiser, N. Esser, F. Bechstedt and A. Pucci, J. Phys. Chem. Lett. 6 (2015) 3615.

First-principles calculations of Au-induced wire structures on Ge(001) surfaces: New atomic models for higher Au coverages

Kaori Seino[a], Friedhelm Bechstedt[b], Simone Sanna[a] and Wolf Gero Schmidt[a]

[a]Lehrstuhl für Theoretische Physik, Universität Paderborn, Paderborn, Germany
[b]Institut für Festkörpertheorie und -optik, Friedrich-Schiller-Universität Jena, Jena, Germany

One-dimensional (1D) electronic systems have been investigated extensively because of the interest both in fundamental physics and in nano or atomic scale devices. Self-assembled atomic scale nanowires provide ideal systems for studying peculiar properties of 1D electronic systems. The Au-induced nanowires on Ge(001) are of particular interest in this respect since they are claimed to host a Luttinger liquid [1]. Despite intense research the microscopic atomic structure of Au-induced nanowires on Ge(001) substrates is still under discussion.

We have studied the structural, energetic and electronic properties of Au-induced nanowires on Ge(001) surfaces by means of density functional theory (DFT) calculations studying the p(4x2) but also p(4x4) and c(8x2) translational symmetries [2,3]. We start the investigations from the original [4] and a modified giant missing row (GMR) structure, the Au-trimer stabilized Ge ridge model [5]. Three new structures (shown in Fig. 1) for a higher Au coverage in the range between 1.25 monolayer (ML) and 1.75 ML are proposed and compared with experimental results [2]. Comparing the relative formation energies the new models are shown to be energetically more favorable than the GMR model proposed previously for lower coverages. Indeed, additional Au atoms at the wire surface stabilize novel geometries. The new models are able to explain several features of the nanowire structure observed by scanning tunneling microscopy and the electronic states found experimentally by angle-resolved photoemission spectroscopy.

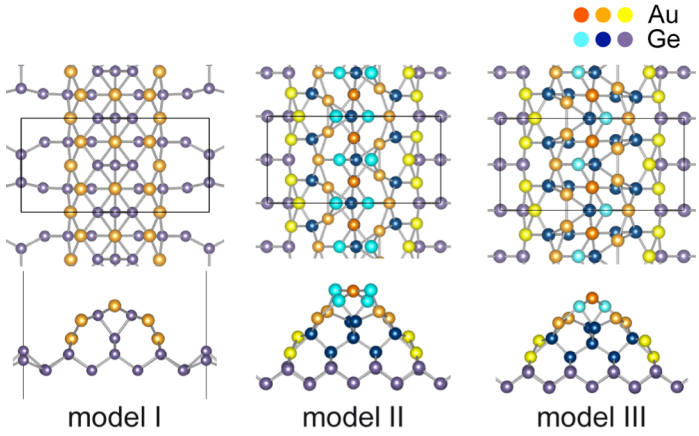

Fig. 1. Proposed structures of the Au/Ge(001) atom chains.

Keywords: Metallic nanowires; Semiconductor surfaces; Density functional theory

References

[1] C. Blumenstein, J. Schäfer, S. Mietke, S. Meyer, A. Dollinger, M. Lochner, X.Y. Cui, L. Patthey, R. Matzdorf, and R. Claessen, Nat. Phys. 7 (2011) 776.
[2] K. Seino and F. Bechstedt, Phys. Rev B 93 (2016) 125406.
[3] K. Seino and F. Bechstedt, J. Phys.: Condens. Matter 28 (2016) 284005.
[4] A. van Houselt, M. Fischer, B. Poelsema, and H.J.W. Zandvliet, Phys. Rev. B 78 (2008) 233410.
[5] S. Sauer, F. Fuchs, F. Bechstedt, C. Blumenstein, and J. Schäfer, Phys. Rev. B 81 (2010) 075412.

COINCIDENCE LATTICES AND INTERLAYER TWIST FOR OPTIMAL VAN DER WAALS HETEROSTRUCTURES

Daniel S. Koda[a], Friedhelm Bechstedt[b], Marcelo Marques[a] and Lara K. Teles[a]

[a]Grupo de Materiais Semicondutores e Nanotecnologia, Instituto Tecnológico de Aeronáutica, DCTA 12228-900, São José dos Campos, Brazil
[b] Institut für Festkörpertheorie und -optik, Friedrich-Schiller-Universität, Max-Wien-Platz 1, D-07743 Jena, Germany

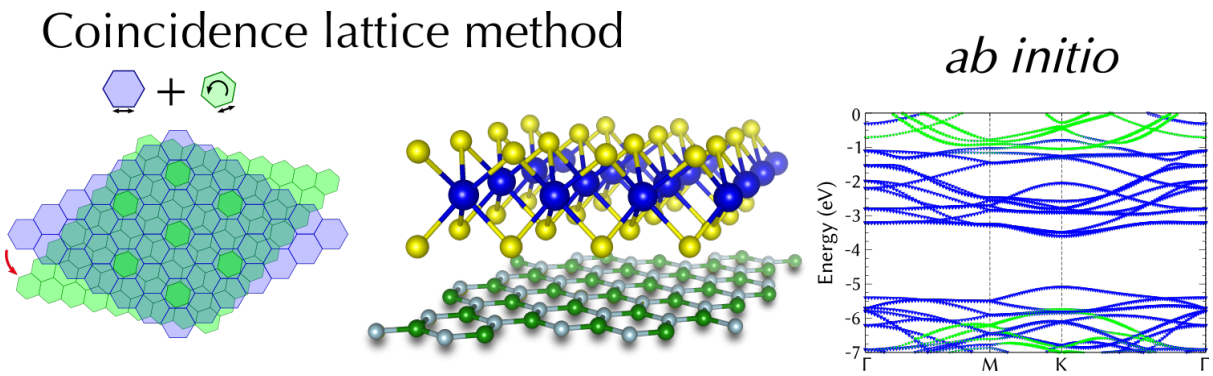

Fig 1: Coincidence lattice method applied on 2D crystals for predictions of vdW heterostructures and *ab initio* calculations.

Van der Waals heterostructures have great potential in large-scale integration devices and new physics exploration. Experimental investigations allow flexible combinations of 2D crystals in device fabrications. Theory, however, has limitations of supercell sizes and commensurability, translated into computational effort. In this work, we demonstrate the application of the coincidence lattice method [1] to simulate two hBN/$MoSe_2$ heterobilayers taking interlayer twist effects into account. We predict that both systems are stable upon contact and interact via van der Waals dispersions. We found that electronic properties of $MoSe_2$ are preserved for both simulated systems, but hBN suffers from the increase of interface interactions, which are evidenced by band structures and density of states calculations. Finally, band discontinuities are obtained and charge transfer arguments explain small shifts in band offsets with respect to natural alignments. We conclude that hBN is a reasonable substrate for maintaining useful properties of $MoSe_2$ for application in electronic and optoelectronic devices and that interlayer twist angles play a significant role in the physics of van der Waals heterostructures.

Keywords: hBN, $MoSe_2$, coincidence lattices method, interlayer twist, vdW heterostructures.

References

[1] D. S. Koda, F. Bechstedt, M. Marques, L. K. Teles. *J. Phys. Chem. C* **120**, 10895 (2016).

MODEL DIFFICULTIES FOR PREDICTING THE POLARIZATION SENSITIVE REFLECTED SECOND HARMONIC GENERATION

C. Emminger[a], C. Reitböck[a,b], J.-P. Perin[a,b], K.-D. Bauer[a,b], A. Alejo-Molina[c], D. Stifter[a,b], K. Hingerl[a]

[a]Center for Surface- and Nanoanalytics, J. Kepler University, Altenbergerstr. 69, 4040 Linz, Austria
[b]Christian Doppler Laboratory for Microscopic and Spectroscopic Material Characterization, J. Kepler University, Altenbergerstr. 69, 4040 Linz, Austria
[c]Center for Research in Engineering and Applied Science (CIICAp), Institute for Research in Pure and Applied Science (IICBA), UAEM Cuernavaca, Mor. 62209, Mexico

In a recent paper from our laboratory we presented the measured second harmonic generation (SHG) response for arbitrarily oriented linear input polarization on Si(111) surfaces in rotational anisotropy experiments[1]. Despite the silicon bulk does not contribute via a dipole transition to SHG, the measured polarization dependent experimental data can only be explained by coherently summing the dipole allowed surface and the quadrupolar bulk SHG sources.

In this contribution we explain the major electrodynamic model aspects for predicting the polarization and intensity response – for clarity we list them with bullet points:

1. First we calculate the strength and direction of the fundamental macroscopic electric field in the material by employing Fresnel's and Snell's laws.

2. The second harmonic polarizability induced ***by the surface dipole*** (C_{3V}-symmetry) can then be calculated by $P_i^s(2\omega) = \varepsilon_0 \sum_{j,k} \chi_{ijk}^{(D)} E_j(\omega) E_k(\omega)$ using a 3rd rank tensor.

3. The second harmonic polarizability induced ***by the bulk quadrupole*** (O_h^7, at any bulk position) can be calculated by $P_i^b(2\omega) = \varepsilon_0 \sum_{j,k,l} \chi_{ijkl}^{(Q)} E_j(\omega) \nabla_k E_l(\omega)$ using a 4th rank tensor.

4. Despite group theory tells that the surface ($\chi_{ijk}^{(D)}$) as well as the bulk tensor ($\chi_{ijkl}^{(Q)}$) have four independent elements, we can analytically prove that for SHG these are reduced to two independent (possibly complex) elements for each of them.

5. In order to handle still less tensor coefficients, we apply the simplified bond hyperpolarizability model (SBHM)[2], which provides for bulk one, for the surface two independent (for one up and three down bonds) tensor coefficients.

6. Because the bulk second harmonic polarization is produced at any depth in the sample and in reflection coherently superimposed at the surface we either fit or analytically calculate (with the given linear dielectric function) the coherent superposition of all bulk waves at the surface. This provides a 4th fit parameter, which can for some physical situations be directly computed.

7. We then discuss the problem of the longitudinal polarizability component, i.e. $\vec{P}(2\omega) \cdot \vec{k}(2\omega) \neq 0$, which occurs for all mentioned tensors at the surface and in the bulk, and how all three polarizability components are transferred to electric ***far-fields*** measurable in the outside by the experimental setup.

8. Finally, we discuss an *ab-initio ansatz*[3] based on density functional theory for predicting the quadrupole contribution of the quantum mechanical response from Bloch functions.

Summarizing, we have implemented steps 1-7 in a forward simulation code and are currently working on a fit program for these 3-4 (complex) parameters.

[1] C. Reitböck, D. Stifter, A. Alejo-Molina, K. Hingerl and H. Hardhienata, J. Opt. **18**, 035501 (2016)
[2] G. D. Powell, J.-F. Wang and D. E. Aspnes, Phys. Rev. **B65**, 205320 (2002)
[3] K.-D. Bauer, M. Panholzer and K. Hingerl, Phys. Status Solidi **B253**, 234-240 (2016)

AB-INITIO INVESTIGATION OF RARE-EARTH SILICIDE THIN FILMS ON SI(111)

C. Dues, W. G. Schmidt and S. Sanna

Department Physik, Universität Paderborn, 33095 Paderborn

Rare-earth (RE) silicide thin films grown on silicon surfaces are currently of high interest. They grow nearly defect-free on different surface orientations because of the small lattice mismatch, and exhibit very low Schottky barriers on n-type silicon. Moreover, they give rise to the self-organized formation of RE silicide nanowires on $\mathrm{Si}(001)$ and vicinal surfaces.

Depending on the amount of deposited RE atoms, a plethora of silicide reconstructions is observed on the $\mathrm{Si}(111)$ surface. While silicide structures occuring in the submonolayer regime show 5×2 and $2\sqrt{3}\times2\sqrt{3}\,\mathrm{R30°}$ periodicities, one monolayer thick silicides crystallize in a phase with 1×1 periodicity, and several monolayer thick silicides lead to a $\sqrt{3}\times\sqrt{3}\,\mathrm{R30°}$ superstructure.

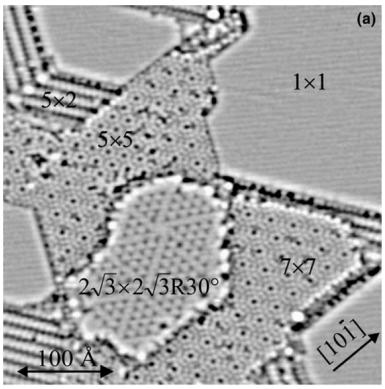

Fig. 1: STM overview images of submonolayer Dy-silicide thin film structures [2].

In this work [1] we investigate the formation of RE silicide thin films on $\mathrm{Si}(111)$ within the density functional theory. We show by ab-initio thermodynamics the occurrence of structures with different periodicity depending on the RE availability and thus reproduce the experimental findings. We calculate structural properties, electronic band structures and compare measured and simulated STM images for each of the silicide phases. Finally, we examine a recent suggestion of a $2\sqrt{3}\times\sqrt{3}\,\mathrm{R30°}$ reconstruction, which is the basis to explain the observation of spot-splitting in SPA-LEED, while STM measurements show no differences compared to the known $\sqrt{3}\times\sqrt{3}\,\mathrm{R30°}$ reconstruction. The calculations are performed with Dy as prototypical RE, but can be extended to other rare-earth elements because of their chemical similarities.

Keywords: Rare Earth Silicide, Si(111), DFT

References

[1] S. Sanna, C. Dues, W. G. Schmidt, F. Timmer, J. Wollschläger, M. Franz, S. Appelfeller, M. Dähne, Phys. Rev. B **93** (2016), 195407.

[2] I. Engelhardt, C. Preinesberger, S.K. Becker, H. Eisele, M. Dähne, Surf. Sci. **600** (2006), 755.

TOWARDS EFFICIENT PLASMONIC EXCITATION OF METAL NANO-ANTENNAS AS AN EFFECTIVE TOOL FOR TIP-ENHANCED RAMAN SPECTROSCOPY

A. Mukherjee[a], E. Sheremet[a], R.D. Rodriguez[b], M. Hietschold[a], D.R.T. Zahn[b]

[a] Solid Surfaces Analysis group and [b] Semiconductor Physics group,
Technische Universität Chemnitz, Germany

Optical nano-antennas exploit the unique properties of metal nanostructures to increase the efficiency of light-matter interaction in important applications such as nanospectroscopy [1]. They may act as near-field optical probe interacting locally with a sample surface due to its ability to focus light at the nanometer scale for imaging beyond the diffraction limit of light *e.g.* in tip-enhanced Raman spectroscopy (TERS) [2, 3]. Efficient excitation of these plasmon-active noble metal probes is a beneficiary factor to boost TERS performance that we report in this work. We implement an efficient local excitation of plasmons selectively at the probe apex by destructive interference in a patterned SiO_2/Si substrate. As a result we determine the resonance conditions for localized surface plasmons (LSPs) by plasmon modulated photoluminescence (PL) [4]. In the second part of this work we report a significant Raman signal enhancement from the substrate as a result of interference-enhanced Raman spectroscopy (IERS) [5]. Additionally, the sample structure allows to reconstruct the geometry and radius of the probe that gives an all in one ultimate and effective method to design tips for nanospectroscopy and tip-enhanced nano-optics.

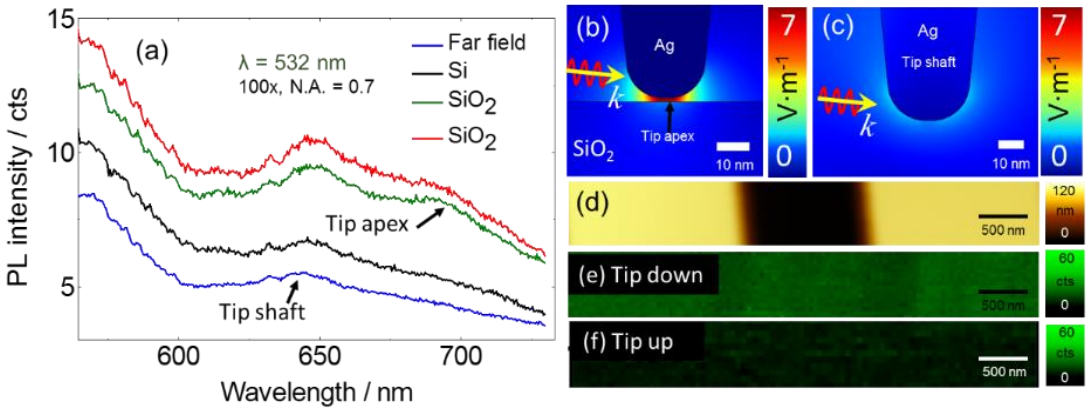

Figure 1: Left: (a) Photoluminescence background for a gold tip above SiO2/Si and without substrate (far field). Right: (b) FEM simulations for spatial distribution of electric field of gold (Au) tips in contact with sample and (c) not in contact with the substrate, (d) AFM topography of the SiO2/Si sample, (e) and (f) TERS images of the Si intensity (at 520.7 cm^{-1}) for tip up and tip down shown at the bottom.

Keywords: Tip-enhanced Raman spectroscopy, interference-enhanced Raman spectroscopy, metal optical nano-antennas, destructive interference.

References:

[1] P. Bharadwaj, B. Deutsch, L. Novotny, Adv. Opt. Photon., 1 (2009) 438-483.

[2] R.M. Stöckle, Y.D. Suh, V. Deckert, R. Zenobi, Chemical Physics Letters, 318 (2000) 131-136.

[3] E. Sheremet, R.D. Rodriguez, A.L. Agapov, A.P. Sokolov, M. Hietschold, D.R. Zahn, Carbon, 96 (2016) 588-593.

[4] E. Dulkeith, T. Niedereichholz, T. Klar, J. Feldmann, G. Von Plessen, D. Gittins, K. Mayya, F. Caruso, Physical Review B, 70 (2004) 205424.

[5] G. Connell, R.J. Nemanich, C. Tsai, Applied Physics Letters, 36 (1980) 31-33.

HYDROGENATION OF SILICENE PHASES ON Ag(111)

D. Solonenko[a], V. Dzhagan[a], D.R.T. Zahn[a], and P. Vogt[a,b]

[a]Institut für Physik, Reichenhainer Str. 70, Technische Universität Chemnitz, D-09126 Chemnitz, Germany
[b]Institut für Festkörperphysik, Hardenbergstraße 36,Technische Universität Berlin, D-10623 Berlin, Germany

New elemental two-dimensional materials, such as silicene, are anticipated to show a greater tunability of their electronic properties in contrast to graphene [1]. This is ensured by a higher sensitivity of their properties to structural modifications [2]. For instance, a band gap opening in silicene can be realized by the adsorption of various atomic species, *i.e.* by functionalization [3], or by applying an electric field normal to its lattice [4].

The adsorption of atomic hydrogen on epitaxial silicene on Ag(111) is studied by *in situ* Raman spectroscopy to monitor the structural and electronic modifications upon hydrogenation. The Raman spectra of the hydrogenated silicene give rise to new Raman modes not yet observed, neither for epitaxial silicene nor any other Si allotropes (including polysilanes [7]). Based on the polarization dependence of these modes, which are in agreement with the C_{3v} symmetry of hydrogenated silicene, we determine the approximate patterns of the atomic motion. The hydrogenation was also performed for the different existing phases of epitaxial silicene on Ag(111) exhibiting different Raman spectra. The hydrogenation behavior also depends on the initial silicene phase confirming the results reported in [5,6]. Despite the apparent effect of the hydrogenation on the silicene structure as judged from the Raman spectra and the univocal theoretical predictions of the band gap opening in silicene via hydrogenation, this effect cannot be unambiguously proved by our study, particularly since no photoluminescence was observed. This can be explained by the interaction with the underlying substrate due to either hybridization of the electronic states, or charge transfer to the metal. The hydrogenation of epitaxial silicene on Ag(111) is largely reversible. Upon heating to 230°C the Raman modes of the initial epitaxial silicene layer can almost be recovered. This implies a rather weak bonding of the H atoms to the Si lattice and contrasts the concept of covalent bonding. Consequently, the hydrogenation also does not improve the resistivity of epitaxial silicene to oxidation. Possible capping strategies to prevent silicene from oxidation will be discussed.

Keywords: Epitaxial silicene; Raman spectroscopy; Hydrogenation

References

[1] D. Jose and A. Datta, Acc. Chem. Res. 47, (2014) 593.
[2] B. Huang, H. J. Xiang, and S.-H. Wei, Phys. Rev. Lett. 111, (2013)145502.
[3] T. H. Osborn, A. A. Farajian, O. V. Pupysheva, *et al.*, Chem.Phys. Lett. 511, (2011) 101.
[4] Z. Ni, Q. Liu, K. Tang, J. Zheng, *et al.*, Nano Lett. 12, (2012) 113.
[5] J. Qiu, H. Fu, Y. Xu, A. I. Oreshkin, *et al.*, Phys. Rev. Lett. 114, (2015) 126101.
[6] W. Wang, W. Olovsson, and R. I. G. Uhrberg, Phys. Rev. B 93, (2016) 81406.
[7] P. Vora, S. A. Solin, and P. John, Phys. Rev. B 29, (1984) 3423.

Surface Structure of Semicrystalline Naphthalene Diimide-Bithiophene Copolymer Films Studied with Atomic Force Microscopy

M. Zerson[a], M. Neumann[a], R. Steyrleuthner[b], D. Neher[b] and R. Magerle[a]

[a]Fakultät für Naturwissenschaften, Reichenhainer Str. 70 09126 Chemnitz, Technische Universität Chemnitz, Germany

[b]Institute of Physics and Astronomy, Karl-Liebknecht-Str. 24/25 14476 Potsdam-Golm, University of Potsdam, Germany

The crystallization behavior, the surface structure, and the nanomechanical properties of a semiconducting polymer play a crucial role in understanding the charge injection process, the transport of the charge carriers, and the processability of the material. Here we study the semiconducting copolymer poly([N,N′-bis(2-octyldodecyl)-11-naphthalene-1,4,5,8-bis(dicarboximide)-2,6-diyl]-alt-5,5′-(2,2′-12 bithiophene)) (P(NDI2OD-T2)) and investigate the influence of annealing conditions on its surface structure through intermittent contact mode atomic force microscopy (AFM) and AFM-based measurements of amplitude-phase-distance (APD) curves.

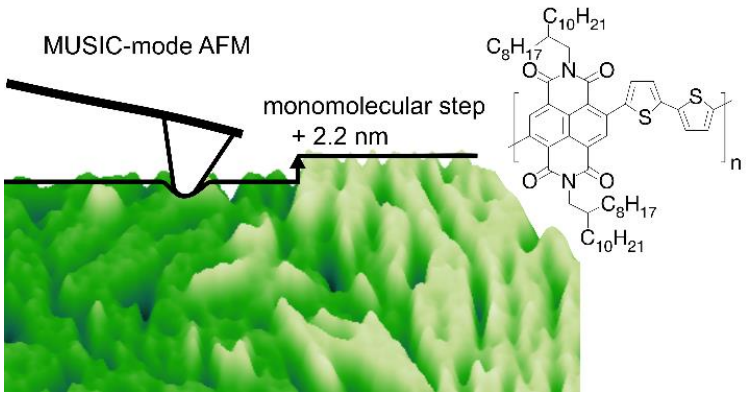

For spin-cast thin films as well as for films annealed at temperatures up to 320 °C, we find that the edges of crystalline lamellae are exposed at the surface. A 1.2-nm-thick layer of alkyl side chains covers the film surface as indicated by the tip indentation. This suggests that charge injection into P(NDI2OD-T2) films is not hindered by a surface layer of amorphous material.

In 5-nm-thick films, corresponding to two monolayers of P(NDI2OD-T2), after annealing at 320 °C, crystalline lamella also orient perpendicular to the film plane with the (100) surfaces oriented parallel to the film plane. The lamellae form ~100-nm-large areas (terraces) with uniform lamella height. The step height between adjacent terraces is 2.2 nm, and we attribute it to monomolecular steps between the molecular-thin layers of edge-on-oriented polymer chains. This well-defined molecular conformation at the film surface with the chain backbone and the π-stacking direction oriented in the film plane is presumably an important factor contributing to the exceptional performance of P(NDI2OD-T2) in bottom-gate organic field-effect transistors.

Keywords: Naphthalene Diimide Copolymer; Semiconducting Polymers; Nanomechanical Properties; Dynamic Atomic Force Microscopy

ELECTRONIC AND STRUCTURAL PROPERTIES OF FERECRYSTALLINE COMPOUNDS INVESTIGATED BY PHOTOELECTRON SPECTROSCOPY

Fabian Göhler[a], Gavin Mitchson[b], Matti Alemayehu[b], Florian Speck[a], Martina Wanke[a], David C. Johnson[b], and Thomas Seyller[a]

[a]Institut für Physik, TU Chemnitz, Reichenhainer Str. 70, D-09126 Chemnitz, Germany

[b]Department of Chemistry and Materials Science Institute, University of Oregon, Eugene, Oregon 97403, United States

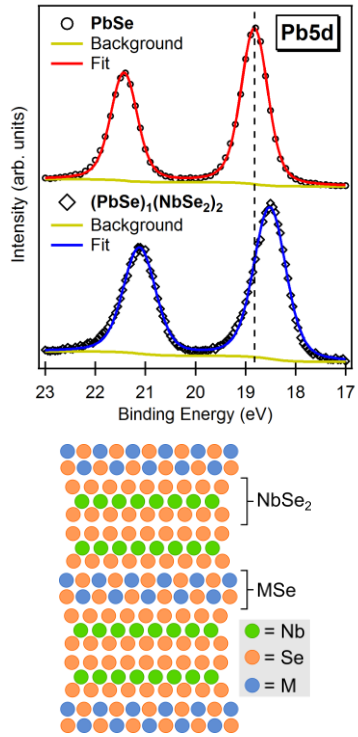

Fig. 1. ***Top:*** XPS Pb5d spectra of a $(PbSe)_1(NbSe_2)_2$ ferecrystal and binary PbSe. ***Bottom:*** Schematic representation of the structure of a $(MSe)_1(NbSe_2)_2$ ferecrystal.

The groundbreaking work on graphene by Novoselov and Geim [1] sparked a run on 2D materials. A combination of different sheet-like materials offers new possibilities in materials properties. The method of *modulated elemental reactants (MER)* [2] enables the preparation of designed turbostratically disordered intergrowths of 2D materials, termed *ferecrystals* [3].

In this work, we investigated the electronic structure of several $(MSe)_1(NbSe_2)_2$ ferecrystals using X-ray photoelectron spectroscopy (XPS). Core level and valence band spectra of ferecrystals with M = Pb or Sn were compared to their respective MER-produced binary compounds MSe and $NbSe_2$. We found evidence of inter-layer interactions and charge transfer as Pb and Sn core levels shift towards lower binding energies in the ferecrystal (Fig. 1).

With XPS, we could also confirm a decrease in the number of antiphase boundaries in $(BiSe)_1(NbSe_2)_n$, when the spacing between the BiSe layers is increased from n = 1 to 2 layers of $NbSe_2$. Antiphase boundaries are a structural modulation occurring in compounds with M = Bi, where Bi-Se bonds are periodically substituted by Bi-Bi bonds [4] (Fig. 2).

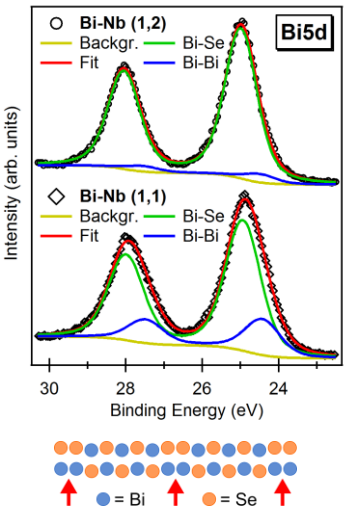

Fig. 2. XPS Bi5d spectra of two $(BiSe)_1(NbSe_2)_n$ ferecrystals with different layer stacking (short Bi-Nb (1,n)). The number of Bi-Bi bonds at antiphase boundaries (red arrows) decreases for n=2.

Keywords: Ferecrystals; Layered Compounds; XPS; Charge Transfer

References

[1] K. S. Novoselov et al., Science 306 (2004) 666.
[2] D. C. Johnson, Curr. Opin. Solid State Mater. Sci. 3 (1998) 159.
[3] M. Beekman et al., Semicond. Sci. Technol. 29 (2014) 064012.
[4] G. Mitchson et al., Inorg. Chem. 54 (2015) 10309.

Stability of GaSe Monolayers

Mahfujur Rahaman*[a], Raul D. Rodriguez[a], Manuel Monecke[a], Santos A. Lopez-Rivera[b], Dietrich R.T. Zahn[a]

[a]Semiconductor Physics, Technische Universität Chemnitz, 09126 Chemnitz, Germany.
[b]Laboratorio de Fisica Aplicada, Universidad de Los Andes, Merida 05101, Venezuela

Two-dimensional (2D) van der Waals semiconductors have been the subject of intense research due to their ultra-low dimension and tunable optoelectronic properties. GaSe (a typical metal monochalcogenides, MMC; MX: M = Ga, In; X = S, Se, Te) belongs to that class of semiconductors and it is of growing interest owing to its optoelectronic properties. However, monolayer stability of this material is one of the important question that needs to be clarified, especially for technological applications. Drapak *et al*. showed that a layer of native oxide forms on a cleaved surface of a bulk GaSe crystal due to storage in air for prolonged time [1. Very recently, the degradation of optical properties of few nm thick GaSe was reported by Zamudio *et al*. [2] while Beechem *et al*. [3] studied the physical process of degradation in GaSe of thicknesses varying from 4 nm to few hundred nm. But environmental stability of GaSe over time is still remained unknown. Here the time stability of GaSe monolayer was investigated by Raman spectroscopy, X-ray photoemission spectroscopy (XPS), phase imaging in dynamic atomic force microscopy, and surface potential mapping. Raman spectroscopy study shows that GaSe monolayers survive only for 5 hours. After that period, GaSe single-layers decomposed into amorphous Se, which is also a good agreement with XPS results. The surface potential study showed GaSe completely passivated by oxidation after 12 hours. The present study provides a clear picture of the monolayer stability in air and will guide future research of GaSe from single- to few-layers in the developing of novel technological applications.

Keywords: 2D materials, GaSe, monolayer stability, oxidation

References

[1] Drapak S. I., Gavrylyuk S. V., Kovalyuk Z. D. & Lytvyn O. S. *Semiconductors* 42 (2008) 414
[2] Pozo-Zamudio O. D., Schwarz S., Sich M., Akimov I. A., Bayer M., Schofield R. C., Chekhovich E. A., Robinson B. J., Kay N. D., Kolosov O. V., Dmitriev A. I., Lashkarev G. V., Borisenko D. N., Kolesnikov N. N. & Tartakovskii A. I. *2D Materials* 2 (2015**)** 035010.
[3] Beechem T. E., Kowalski B. M., Brumbach M. T., Mcdonald A. E., Spataru C. D., Howell S. W., Ohita T., Pask J. A. & Kalugin N. G. *Applied Physics Letters* 107 (2015) 173103.

SPECTROSCOPIC ELLIPSOMETRY STUDIES OF $TlIn(S_{1-x}Se_x)_2$ SOLID SOLUTIONS AT DIFFERENT TEMPERATURES

O.O. Gomonnai[a], O. Gordan[b], P.P. Guranich[a], A.V. Gomonnai[c], A.G. Slivka[a], D.R.T. Zahn[b]

[a] Uzhhorod National University, 46 Pidhirna Str., 88000 Uzhhorod, Ukraine
[b] Semiconductor Physics, Technische Universität Chemnitz, 70 Reichenhainer Str., D-09107 Chemnitz, Germany
[c] Institute of Electron Physics, Ukr. Nat. Acad. Sci., 21 Universytetska Str., 88017 Uzhhorod, Ukraine

$TlInS_2$-type crystals are layered ferroelectric semiconductors with a complex sequence of structural phase transformations including incommensurate phase in the interval 201–216 K [1]. Besides, a Lifshitz-type point is possibly observed in the (x, T) phase diagram of $TlIn(S_{1-x}Se_x)_2$ solid solutions at x = 0.05 [2].

Here we report on ellipsometry studies for $TlIn(S_{1-x}Se_x)_2$ solid solutions at different temperatures. $TlIn(S_{1-x}Se_x)_2$ (x = 0, 0.05, 0.08, 0.25) single crystals were obtained by Bridgman technique. The real ε_1 and imaginary ε_2 parts of the dielectric function of the $TlIn(S_{1-x}Se_x)_2$ single crystals were obtained in the 1 to 5 eV spectral range in the (001) layer plane. Temperature studies of energy dependences of ε_1 and ε_2 in the temperature range 143-293 K were performed using a Linkam stage THMS600.

The measured ε_1 and ε_2 spectra exhibit several optical features associated with interband transition critical points (CPs). Their energies were determined by analyzing the calculated second-energy derivatives of functions obtained from the ellipsometric measurements.

Analysis of the second derivative spectra of the dielectric function at room temperature in the above-bandgap region revealed the presence of four critical points at E_{c1} = 3.24 ± 0.01 eV, E_{c2} = 3.33 ± 0,01 eV, E_{c3} = 3.59 ± 0.01 eV and E_{c4} = 4.52 ± 0.05 eV for $TlInS_2$, five critical points at E_{c1} = (3.24±0.01) eV, E_{c2} = (3.32±0.02) eV, E_{c3} =(3.60±0.01) eV, E_{c4} = (4.25±0.1) eV, and E_{c5} = (4.39±0.1) eV for $TlIn(S_{0.95}Se_{0.05})_2$, E_{c1} = (3.25±0.01) eV, E_{c2} = (3.30±0.02) eV, E_{c3} =(3.61±0.01) eV, E_{c4} = (4.27±0.3) eV, and E_{c5} = (4.36±0.3) eV for $TlIn(S_{0.92}Se_{0.08})_2$ as well as six critical points at E_{c1} = (2.68±0.01) eV, E_{c2} = (2.88±0.05) eV, E_{c3} = (3.49±0.5) eV, E_{c4} = (3.51±0.5) eV, E_{c5} = (3.65±0.2) eV, and E_{c6} = (4.31±0.2) eV for $TlIn(S_{0.75}Se_{0.25})_2$ crystal.

Temperature dependences of interband transition energies for $TlIn(S_{1-x}Se_x)_2$ crystals are discussed.

Keywords: ferroelectric; dielectric function; critical point

References

[1] A. M. Panich, J. Phys. Condens. Matter. 20 (2008) 293202
[2] M.-H.Yu. Seyidov, R.A. Suleymanov, and F. Salehli, Phys. Solid State. 51 (2009) 2513.

BRIGHTLY LUMINESCENT COLLOIDAL Ag-In-S NANOPARTICLES STABILIZED IN AQUEOUS SOLUTIONS BY BRANCHED POLYETHYLENEIMINE

A. Raevskaya, M. Ivanchenko, O. Stroyuk

L.V. Pysarzhevsky Institute of Physical Chemistry of Nat. Acad. Sci. of Ukraine, prosp. Nauky 31, Kyiv 03028, Ukraine

A direct and mild synthesis of water-soluble brightly luminescent Ag-In-S nanoparticles (NPs) stabilized by branched polyethyleneimine (PEI) is proposed. The key parameters influencing spectral parameters and photoluminescence (PL) intensity of Ag-In-S NPs are (i) the Ag:In and Ag:S ratios and (ii) duration of the post-synthesis thermal treatment of colloidal solutions at ~100 °C. A variation of the Ag:In ratio allows to tune the PL color from green to orange-red (Fig. 1). The maximal PL quantum yield, 20%, was observed for the Ag-In-S-PEI NPs produced at a molar Ag:In:S ratio of 1:5:5 and 2-h post-synthesis thermal treatment at around 100 °C. Dynamic light scattering showed that such NPs have an average hydrodynamic size of ~100 nm. According to SEM each 100-nm globule comprises many separate smaller Ag-In-S NPs. Reasonably high PL quantum yield, variability of the emission color and self-aggregation of Ag-In-S-PEI NPs into polymer globules that do not scatter light makes such NPs promising for the luminescent bio-labeling applications. The PL band maximum energy of the Ag-In-S-PEI NPs produced in optimal conditions is very close to the band gap derived from the absorption spectra of colloidal solutions indicating that the PL originates either from the radiative recombination between delocalized conduction band electron and valence band hole or from the radiative recombination with the participation of the charge carriers captured by “shallow” traps. A large spectral width of the PL bands of Ag-In-S-PEI NPs can be interpreted as a result of size distribution of NPs residing in a regime of strong spatial exciton confinement.

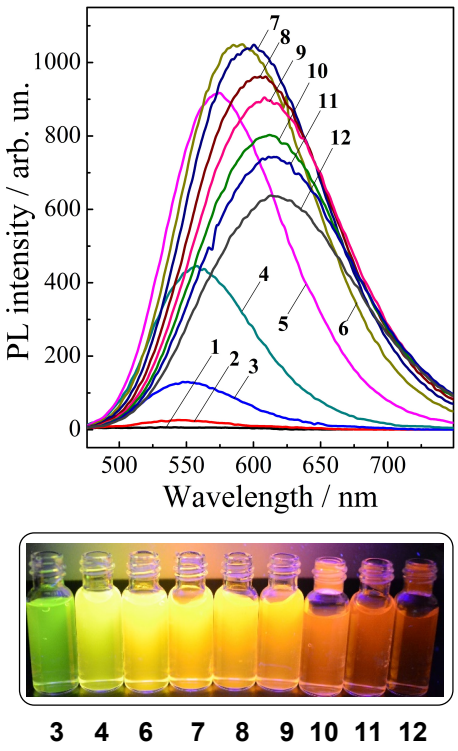

Fig. 1. PL spectra and photographs of colloidal Ag-In-S NPs synthesized at Ag:In:S ratio = x:5:5, x = 0.1 (curve 1), 0.2 (2), 0.3 (3), 0.5 (4), 0.7(5), 0.9 (6), 1.0 (7), 1.1 (8), 1.2 (9), 1.3 (10), 1.4 (11), and 1.5 (12). PL was excited at λ = 450 nm. Photographs were taken under UV illumination (350-400 nm).

The work is supported by the Volkswagen Foundation (project “New functionalities of semiconductor nanocrystals by controllable coupling to molecules”).

TEMPERATURE DEPENDENT EXCITON-PHONON COUPLING IN SEMICONDUCTOR CdSe/ZnS QUANTUM DOTS

E. Zenkevich[a], A. Stupak[b], and C. von Borczyskowski[c]

[a]National Technical University of Belarus, Minsk 220013, Belarus
[b]B.I. Stepanov Institute of Physics, 220072 Minsk, Belarus
[c]Institute of Physics, Chemnitz University of Technology, 09107 Chemnitz, Germany

One long standing question in semiconductor quantum dots (QDs) physics is the effect of quantum confinement on the strength of exciton-phonon coupling (EPC) and phonon frequency, a topic that has received considerable experimental and theoretical attention. Upon evaluation of EPC parameters for QDs, the majority of previous temperature experiments have been carried out for QDs dissolved in rigid matrixes (polymers, resins, *etc*.). In this report, we will discuss temperature dependent exciton-phonon coupling in CdSe/ZnS QDs capped by TOPO ligands and embedded into a glass forming liquid. In the later case, a possible phase transition of the capping ligand layer should be taken into account.

While in most reported experiments photoluminescence (PL) data (PL energy; PL band width, or Stokes shifts) have been used to determine EPC parameters we used in parallel temperature dependent absorption data which provided in combination with PL emission the identification of the temperature dependence of the Stokes shift, which in return reveals temperature dependent Huang-Rhys factors. We found that temperature dependent data from absorption are slightly but definitely different from those obtained by PL. We explained this finding by the analysis that absorption is more sensitive to core CdSe LO optical phonons while PL also contains coupling to ZnS phonons of the shell. In addition, as we shown recently [1] PL emission of QD is to a large extent due to QD surface states. A phase transition-type changes were found in absorption and PL. From the temperature dependent Stokes shift analysis it was elucidated that EPC below the phase transition temperature T_{crit} is governed more efficiently by coupling to ZnS phonons, while above coupling to CdSe increases. This result is supported by the observation that the (size dependent) phase transition appears at lower temperatures (≈ -10 K) in absorption (predominant excitation of small QDs) as compared to the one detected in PL from dominantly surface states. It follows from the obtained results that determination of EPC via Stokes shifts needs a temperature dependent investigation to reduce (i) contributions from the thermalization of the excitonic fine structure levels, (ii) influence of differently contributing near-band-edge states and shallow traps and (iii) identification of the "true" first absorption band. Neglecting these influences will result in too large Stokes shifts and exciton-phonon coupling constants.

Finally, the most interesting finding is that contrary to results reported in literature, temperature activated coupling to optical phonons proceeds not via excitation to the second excitonic state but to a recently identified hole state which has often been overlooked in several reported investigations.

Keywords: Semiconductor quantum dots, Ligand dynamics, Photoluminescence, Absorption, Surface traps, Exciton-phonon coupling, Temperature surface "phase" transition.

References

[1] E. Zenkevich, A. Stupak, C. von Borczyskowski, In "Tuning Semiconducting and Metallic Quantum Dots: Spectroscopy and Dynamics" (Eds.: C. von Borczyskowski, E. Zenkevich), Pan Stanford Publishers, Singapore, Chapter 3 (2016, in press).

CONFINED AND INTERFACE PHONONS IN 2D COLLOIDAL NANOCRYSTALS

V.M. Dzhagan[a], A.G. Milekhin[b], S.Pedetti[c], B. Dubertret[c], D. R.T. Zahn[a]

[a]Semiconductor Physics, Reichenhainer Str. 70, D-09107 Chemnitz, Technische Universität Chemnitz, Germany
[b]A.V. Rzhanov Institute of Semiconductor Physics, pr. Lavrentieva 13, 630090 Novosibirsk, Russia
[c]Laboratoire de Physique et d'Etude des Matériaux, CNRS, ESPCI, 10 *rue* Vauquelin, 75005 Paris, France

Recently developed 2D colloidal semiconductor nanocrystals, or nanoplatelets (NPLs) [1], extend the range of solution-processable free-standing nanomaterials of high performance. Growing CdSe and CdS subsequently in either side-by-side or stacked manner results in core-crown or core/shell structures, respectively. Both kinds of hetero-NPLs find efficient applications and represent interesting materials to study the elemental excitations under strong one-directional confinement [2].

Here, we investigated by Raman and infrared spectroscopy the phonon spectra and electron-phonon coupling in CdSe/CdS core/shell and core-crown NPLs. A number of distinct spectral features of the two NPL morphologies are observed, which are further modified by tuning the laser excitation energy E_{exc} between in- and off-resonant conditions. The general difference is the larger number of phonon modes in core/shell NPLs and their spectral shifts with change of shell thickness or E_{exc}. The spectra of the core-crown NPLs are more resembling the sum of spectra of the isolated CdSe and CdS particles, and are similar to spherical morphologies studied earlier. This behaviour is explained by mutual influence of the core and shell in NPLs and formation of combined modes. In the core-crown structure, the CdSe and CdS modes preserve more independent behaviour with only interface modes forming overtones with core phonons.

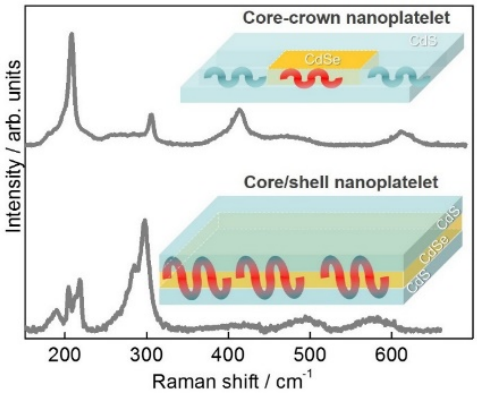

Fig. 1. Representative resonant Raman spectra of two types of CdSe/CdS NPL morphologies shown in the insets.

Keywords: Semiconductor Nanocrystals, Interface, Core-Shell, Phonons, Raman, Infrared

References

[1] S. Ithurria, M. D. Tessier, B. Mahler, R. P. S. M. Lobo, B. Dubertret, A. L. Efros. Nat. Mater. 10 (2011) 936.
[2] A. Antanovich, A. Prudnikau, A. Matsukovich, A. W. Achtstein, M. J. Artemyev, Phys. Chem. C 120 (2016) 5764.

Solid-phase interaction in the bilayer eutectic nanofilms

T. Doroshenko, G. Dorozinsky

V. Lashkaryov Institute of Semiconductor Physics NAS of Ukraine, 41 Nauki ave., 03028 Kyiv, Ukraine

Low-temperature solid-phase interaction in the simple eutectic pairs of metal-semiconductor nanofilms is one of the ways to create new materials for engineering of nanoplasmonic and nanophotonic structures. In present report bilayer systems of semiconductor and metals that are forming simple eutectic pairs Ge-Au, Ag, Al, the changes of structural and optical properties of this bilayer eutectic nanofilms during the laser and thermal annealing were investigated. Bilayer eutectic nanofilm systems were prepared by thermal evaporation in vacuum with computer control technique.

The nanostructure with total thickness 45 - 50 nm and width of pits 0,5mkm was obtained via laser beam treatment of two-layer eutectic system Ge-Au, Ag, Al. The annealing was performed by laser with a wavelength of 530 mkm. The laser annealing power of this structures on glass substrates was 4-11mW [1,2].

The results of bilayer eutectic nanofilms thermal annealing demonstrate the changing of transmission and reflection index. At the same time AFM images of samples before and after the thermal annealing show the same structure. The temperatures of solid-phase interaction of investigating samples was 1,5-3 times less then eutectic temperatures. Spectra of binary mixtures Ge-metals were measured in situ during the thermal annealing. Also be noted that reflection index spectra of the systems Ge-Au,Ag,Al before and after annealing are different [3]. All features of the investigated systems described above can be used for creation photonic crystals.

One of the main elements of the surface plasmon resonance (SPR) technique is SPR biosensor chips (glass plate with 50 nm Au). This paper reports an effective method to enhance the surface plasmon resonance (SPR) on Au films by using a thin Ge layer. Au films with a thickness of about 50 nm were deposited by thermal evaporation in vacuum above an ultrathin Ge layer of ∼2 - 5nm on glass substrates. The surface roughness have been reduced from >5 nm for a pure Au film to ≤1nm for Au/Ge films, respectively Our results show that Ge acts as a roughness-diminishing growth layer for the Au film while at the same time maintaining and enhancing the plasmonic properties of the combined annealling structures. This points toward its use for low-loss plasmonic devices and optical metamaterials applications.

Keywords: bilayer eutectic nanofilms, laser and thermal annealing, surface plasmon resonance, metamaterials, gold, germanium,surface roughness.

References

[1] Doroshenko Tamara, Laser beam irradiation-induced processes in binary films Proc. SPIE 3282 (1998) 71

[2] Doroshenko Tamara, Optical recording on eutectic pairs of thin films Proc. SPIE 3055 (1997) 54

[3] Doroshenko T., Grynko D., Induced processes in binary metal-semiconductor eutectic nano-structured films EMRS 2014 FALL MEETING, Poland,S59 (2014) 278

VIBRATION EIGENMODES OF THE ORDERED ADSORBATE Au-(5X2)/Si(111): RAMAN SPECTROSCOPY AND FIRST-PRINCIPLE CALCULATIONS

B. Halbig[a], M. Liebhaber[a], U. Bass[a], J. Geurts[a], E. Speiser[b], J. Räthel[b], A. Baumann[b], S. Chandola[b], N. Esser[b], S. Neufeld[c], S. Sanna[c], W.G. Schmidt[c]

[a]Physikalisches Institut, Exp. Physik 3, Universität Würzburg, Germany
[b]Leibniz-Institut für Analytische Wissenschaften - ISAS - e.V. - Berlin, Germany
[c]Department Physik, Universität Paderborn, Paderborn, Germany

A sub-monolayer coverage of metal atoms on a semiconductor surface can exhibit a self-assembled reconstruction pattern, inducing electronic correlation effects, especially for one-dimensional chains. These effects are tightly connected with the local arrangement of the atoms and the corresponding vibration eigenmodes. For this purpose, the Au/Si(111) system has found broad interest. Well-defined reconstruction patterns can be induced for appropriate Au coverages and substrate temperatures, e.g. the Au-(5x2) reconstruction, consisting of parallel chains with Au single and double rows. Its vibration eigenfrequencies and mode symmetries can be studied with high spectral resolution by Raman spectroscopy.

We report on polarized *in-situ* UHV Raman spectroscopy of the vibrational eigenmodes of self-assembled Au-structures on Si(111) surfaces, whose (5x2) reconstruction was confirmed by LEED. Although the intensity of the Au- and surface-related Raman signals is about four orders below the Si bulk phonon signal because of their extremely low scattering volume, high-sensitivity CCD detection allows the identification of the Au-induced vibration modes. In the Raman spectrum they replace the peaks which were previously identified as surface vibration modes of the clean (7x7)-reconstructed Si(111) surface [1]. The positions of the Au-induced Raman peaks are in the range between 3 meV and 15 meV, the strongest ones at 3 meV, 6 meV, and 13 meV. These Raman peaks show mode-specific polarization properties, which are strongly correlated with the direction of the Au-induced chains.

Furthermore, we performed first-principles calculations of the Au-(5x2)/Si(111) surface dynamics within Density Functional Theory as implemented in the VASP package. In addition to eigenmodes patterns and eigenfrequencies, we calculated also the Raman scattering efficiencies. This allows the comparison of our experimental results with the calculated vibrations for two currently discussed Au-(5x2) reconstruction models, an intrinsically (5x1) model by Erwin *et al.* [2], which achieves the (5x2) periodicity by invoking a double-periodicity arrangement of Si adatoms along the chains, and alternatively a modified model by Kwon and Kang [3], where one additional Au-atom per unit cell yields a genuine (5x2) periodicity.

Keywords: Au-(5x2)/Si(111), Vibrations, Raman, First-Principle Calculations

References

[1] M. Liebhaber *et al.*, Phys. Rev. B 89 (2014) 045313
[2] S.C. Erwin *et al.*, Phys. Rev. B 80 (2009) 155409
[3] S.G. Kwon and M.H. Kang, Phys. Rev. Lett. 113 (2014) 086101

ATOMICALLY FLAT SURFACE RECONSTRUCTION OF THE Bi_2Te_3 TOPOLOGICAL INSULATOR

U. Thupakula[a], K. Schouteden[a], A. M. Netsou[a], Z. Li[a], T. Chen[b], F. Song[c] and C. Van Haesendonck[a]

[a]Solid-State Physics and Magnetism Section, KU Leuven, BE-3001 Leuven, Belgium
[b]Department of Solid State Chemistry, Max-Planck-Institute for Chemical Physics of Solids, 01187 Dresden, Germany
[b]National Laboratory of Solid State Microstructures, Nanjing University, 210093 Nanjing, P. R. China

Topological insulators (TIs) are materials with an insulating bulk interior and a single, non-degenerate Dirac fermion band on the surface [1]. Of the available TIs bismuth telluride (Bi_2Te_3) has received considerable attention due to its promising applications in spintronics. Bulk Bi_2Te_3 has a layered structure consisting of quintuple layers (QLs) with each QL consisting of a sequence of Te-Bi-Te-Bi-Te atomic planes [2]. This allows for a convenient cleaving between adjacent QLs along the (111) direction. Here, we present the results of our detailed study of the influence of annealing under UHV conditions on surface reconstruction behavior of freshly cleaved Bi_2Te_3. We investigated this surface behavior using UHV scanning tunneling microscopy (STM). We found that there is a gradual change in the surface reconstruction of the Bi_2Te_3 with the annealing temperature (Fig. 1). Additionally, annealing to 400 °C results in an atomically flat surface with an increased density of the atomic steps on the Bi_2Te_3 surface. Moreover, Auger spectroscopy reveals the appearance of a Bi (111) bilayer as the top most layer atop the QLs after annealing at 400 °C, which is further supported by STM height profile measurements. Our systematic investigation may provide a pathway to overcome the difficulties which are associated with complex in-situ surface preparation techniques.

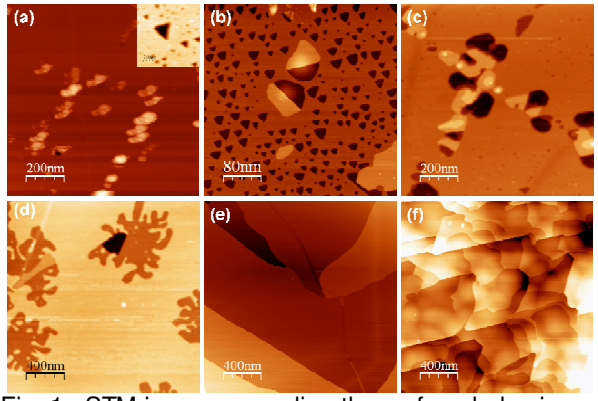

Fig. 1. STM images revealing the surface behavior (a) before the annealing and for different annealing temperatures: (b) 200, (c) 250, (d) 290, (e) 330, and (f) 400 °C under UHV conditions.

Keywords: Bi_2Te_3; Topological Insulator; Scanning Tunneling Microscopy

References

[1] X. L. Qi, T. L. Hughes, S. C. Zhang, Phys. Rev. B 78 (2008) 195424.
[2] D. Teweldebrhan, V. Goyal, A. A. Balandin, Nano Lett. 10 (2010) 1209.

CONTROL OF METALS SULFIDE NANOCRYSTALS GROWTH: MORPHOLOGY AND APPLICATIONS

D. Grynko [a], E. Bortchagovsky [a], V. Styopkin [b], G. Hesser [c]

[a] Institute of Semiconductors Physics, NAS of Ukraine, Kyiv;
[b] Institute of Physics, NAS of Ukraine, Kyiv;
[c].University of Linz, Austria.

Nanocrystals of metals sulphide – NiS, AgS, CdS (NC) are very prospective nanoobjects due to crystalline anisotropy, photoconductive, ferroelectric and magnetic properties of material. Control of NC growth from gaze phase give us ability to change morphology from amorphous or polycrystalline nanowires to single crystal nanoobjects. Its diameter may be in the range of tens and hundreds of nanometres and length – from hundreds nanometres to tens of microns. What is why scanning electron microscopy gives us important information on NC morphology. In our experiments NC are grown from gaze phase in the quasi-closed volume. Design feature of NC growth setup gives us ability to stop the growth of NC and reevaporate it partially.

Value of diffusion length can be measured from NC shape if NC had been grooved when transport is a limiting factor in the chain of NC growth stages. In our experiments diffusion length had the order of microns and it can be controlled by saturation and substrate temperature. Nucleation and crystallization rate relation in the vapor-liquid-solid growth determines shape of the nanowire and its crystallinity. Analysis of growth rate as a function of NC diameter allows us to estimate time of crystallization front propagation and time of nucleation. Nucleation time can be found in the range of seconds. If nucleation time is lower than the time of crystallization front propagation then growth of nanosize monocrystal can be realized in monocentric mode. At the polycentric mode probability of nucleation of a few nucleus is enough during the time of crystallization front propagation. Knowledge of diffusion length, nucleation time and crystallization rate as a function of conditions of growth allows us to control crystallinity and morphology of CdS nanocrystals.

Piezoelectric properties of CdS NC give us ability to design piezoresonance sensors with projective sensitivity in order of 10^{-16}g due to small mass of single NC.

The peculiarity of CdS tripode and tetrapode nanocrystal elements is the fact that under certain conditions of heteroepitaxial growth its geometry is determined by the crystallographic structure of semiconductor substrates what governs the orientation of tripods, and only length is defined by the technological parameters of growth kinetics. Application areas of tripode and tetrapode nanocrystal are: nanoantennas - detectors of radiation, electroluminescent devices, biosensors.

Growth of semiconductor nanocrystals in the microelectrodes space is a self-organizing process suitable for one dimensional devices manufacture as opposed to existing technique of single crystal attaching to microelectrodes by micromanipulator and connecting into electric circuit by electron-beam lithography. Our approach to this problem is based on the use of processes of self-organization of semiconductor nanocrystals, which will allow us to grow nanocrystals with a given morphology, crystallinity, type of lattice and to form the complete device. Application of single nanocrystal element is biosensor which consists of microelectrodes and a one-dimensional single semiconductive nano- crystal connected in the electric circuit.

Keywords: nanocrystal, growth, nucleation, crystallization, SEM, morphology, biosensor